



UNIVERSITY of the
WESTERN CAPE

Discriminative eradication of cancer cells using quantum dots functionalised with peptide-directed delivery of a pro-apoptotic peptide



Lauren Taryn Swartz

UNIVERSITY of the
WESTERN CAPE

A thesis submitted in partial fulfilment of the requirements for the degree
Magister Scientiae in the Department of Biotechnology, University of the
Western Cape.

Supervisor: Dr Mervin Meyer
Co-Supervisor: Dr Martin Onani

December 2013

TABLE OF CONTENTS

Abstract.....	9
Keywords	11
Declaration.....	12
List of Figures.....	13
List of Tables	14
Abbreviations	15
Dedication	17
Acknowledgements	18



1. Chapter One: Literature Review

1.1. Introduction	19
1.2. Cancer development.....	19
1.2.1. Tumour physiology.....	19
1.2.2. Tumour vasculature	20
1.3. Challenges in current cancer therapeutics.....	21
1.4. Targeted drug delivery systems	
1.4.1. Passive targeting	23
1.4.2. Active targeting	23
1.5. Cancer specific peptides as useful targeting agents	
1.5.1. Why peptides?	24
1.5.2. Development of targeting peptides against cancer gene expression patterns	25
1.5.3. The identification of targeting peptides	25
1.5.4. The LTVSPWY peptide	27
1.6. Cancer and apoptosis	
1.6.1. The role of apoptosis in cancer progression	28
1.6.2. Apoptosis pathways	29
1.6.3. The Extrinsic pathway	29
1.6.4. The Intrinsic pathway	30
1.6.5. Pro-apoptotic agents as anti-cancer drugs	30

1.7. Smac/DIABLO: a pro-apoptotic agent

1.7.1. Smac/DIABLO	31
1.7.2. Smac/DIABLO association with inhibitors of apoptosis proteins.....	31
1.7.3. The application of Smac/DIABLO in the treatment of cancer	33

1.8. Nanotechnology-based drug delivery systems

1.8.1. Nanotechnology.....	35
1.8.2. Quantum dots.....	36
1.8.2.1. Optical properties	36
1.8.2.2. Quantum dots versus organic fluorophores	37

1.9. The application of QDs in targeted drug delivery systems

1.9.1. Water-soluble QDs	38
1.9.2. Bi-conjugation chemistry.....	39
1.9.3. Peptide directed QDs	40
1.9.4. Multifunctional QDs for cancer treatment.....	41
1.9.5. Cytotoxicity of QDs.....	42

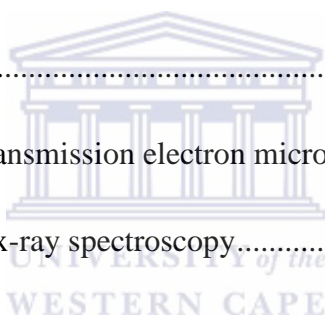
1.10. Objective of this study

43



2. Chapter Two: The synthesis, characterisation and solubilisation of CdSe/ZnS core-shell quantum dots

2.1. Introduction	44
2.2. Objective of this chapter	45
2.3. Materials and Suppliers	46
2.4. Methods	47
2.4.1. The organometallic synthesis of CdSe/ZnS core-shell QDs.....	47
2.4.2. Precipitation of the CdSe/ZnS core-shell QDs	48
2.4.3. Characterisation of the CdSe/ZnS core-shell QDs	49
2.4.3.1. PL spectroscopy	49
2.4.3.2. High Resolution transmission electron microscopy.....	49
2.4.3.3. Energy dispersive x-ray spectroscopy.....	50
2.4.4. Ligand exchange	50
2.5. Results and discussion	51
2.5.1. Synthesis of CdSe/ZnS core-shell QDs	51
2.5.2. Characterisation of CdSe/ZnS core-shell QDs	51
2.5.2.1. Introduction	51
2.5.2.2. PL properties of CdSe/ZnS core-shell QDs	52
2.5.2.3. Transmission electron microscopy.....	54
2.5.2.4. Energy dispersive x-ray spectroscopy.....	55
2.6. Water-soluble CdSe/ZnS core-shell QDs	57
2.6.1. Introduction.....	57



2.6.2. Ligand exchange	57
3. Chapter Three: Selective eradication of cancer cells using peptide directed QDs to deliver a pro-apoptotic peptide	
3.1. Introduction	59
3.2. Objective of this chapter	59
3.3. Materials and Suppliers.....	60
3.4. Solutions and buffers	61
3.5. Methods	61
3.5.1. Cell culture.....	61
3.5.2. Thawing of cells	61
3.5.3. Trypsinization of cells	61
3.5.4. Freezing of cells.....	62
3.6. Dose response curves.....	62
3.6.1. Seeding of cells.....	62
3.6.2. QD Treatment	62
3.7. Bi-conjugation of QDs to peptides	62
3.8. Desalting of the QD peptide bi-conjugates using gel filtration	63
3.9. Immunocytochemistry	64
3.9.1. Seeding of cells.....	64
3.9.2. Fixation and permeabilisation.....	64
3.9.3. Fixed cell staining.....	64
3.9.4. Live cell staining.....	65



3.10. Cytotoxicity assay.....	65
3.11. Results and discussion	67
3.11.1. Dose response curves to determine optimal QD concentration	67
3.11.2. Bi-conjugation of QDs to peptides using EDC chemistry	69
3.11.3. Desalting of the QD peptide bi-conjugates.....	70
3.11.4. Evaluating the cytotoxicity of the QD peptide bi-conjugate targeted drug delivery system using the WST-1 Cell Proliferation assay	71
3.11.5. Evaluating the binding affinity of the QD peptide bi-conjugates.....	75
3.11.6. Evaluating the internalisation of the QD peptide bi-conjugates.....	79



4. Summary of this study..... 84

4.1. General discussion..... 84

4.2. Conclusion..... 88

4.3. Future work 88

4.4. References 90



ABSTRACT

The therapeutic goal of cancer treatment is to trigger selective cell death in cancer cells. To eliminate cancerous cells effectively, the anti-cancer drugs must be targeted to the affected cells. However, anti-cancer drugs are often distributed non-specifically giving rise to systemic toxicities and other adverse effects. Cancer specific peptides are useful cancer targeting agents that can be used for the targeted delivery of anti-cancer drugs. Several cancer targeting peptides and some of their corresponding protein targets have been identified. Previous work investigated the specific binding of five of these peptides (p.C, p.H, p6.1, Frop-1 and p.L) conjugated to fluorescent nanoparticles (quantum dots) to a panel of human cell lines, which included four cancerous cell lines (Caco-2, HeLa, HT29 and HepG2) and one non-cancerous cell line (KMST-6). Flow cytometry showed that the p.L peptide preferentially bind to HT29 cells; suggesting that the expression levels of the target for the p.L peptide are higher in these cells.

The objective of this study was to make use of target specific functionalised quantum dots (QDs) to deliver Second mitochondria-derived activator of caspases/ Direct AIP binding protein with low PI (Smac/DIABLO) to HT29 cells with the aim of enhancing the effects of pro-apoptotic drugs. Smac/DIABLO is a pro-apoptotic peptide that is able to interact with inhibitor of apoptosis proteins (IAPs), thereby inducing pro-apoptotic signalling. *Methodology:* CdSe/ZnS core-shell QDs were synthesised using the one-pot synthesis method. These QDs were characterised using photoluminescence (PL) spectroscopy, high resolution transmission electron microscopy (HR-TEM) and energy dispersive x-ray spectroscopy (EDS). The CdSe/ZnS core-shell QDs were solubilised with L-cysteine (Cys-QDs). The Cys-QDs were bi-conjugated to the p.L peptide and Smac peptide using 1-ethyl-3-(30-dimethylamino) carbodiimide (EDC) chemistry. Cultured HT29 cells were exposed to the

QD peptide bi-conjugates and fluorescence microscopy was employed to assess targeting and internalisation. The cytotoxicity of the QD peptide bi-conjugates in combinatorial treatment with ceramide was evaluated using the WST-1 Cell Proliferation assay. A commercially available QD with similar chemistry was used to carry out a comparative study to relate the efficiency of the in-house synthesized QD.

This study demonstrated that green fluorescent CdSe/ZnS core-shell QDs were successfully synthesised and solubilised. Additionally, the QD peptide bi-conjugates proved to be an ineffective combinatorial treatment and consequently, HT29 cells were not sensitised to ceramide induced cell death. Finally, the microscopy data suggests that the bi-conjugation strategy may have been unsuccessful as demonstrated by no selective targeting to HT29 cells. To evaluate the effectiveness of the drug delivery system developed in this study, alternative bi-conjugation schemes may be investigated. Although the overall objective was not met, the efficiency of the in-house synthesised Cys-QDs in comparison to the standard Qdot525 was observed to be of good quality and therefore, may potentially be used in other biological applications.

KEYWORDS

Apoptosis

Bi-conjugation

Cancer specific peptides

EDC

Fluorescence

Nanotechnology

QDs

Smac/Diablo

Selective killing

Targeted delivery



DECLARATION

I declare that “Discriminative eradication of cancer cells using quantum dots functionalised with peptide-directed delivery of a pro-apoptotic peptide” is my own work that has not been submitted for any degree or examination in any other university and that all the sources I have used or quoted have been indicated and acknowledged by complete references.



Signed:

Date:.....

LIST OF FIGURES

Figure 1.1. Tumour growth from a single cell.

Figure 1.2. Passive versus active targeting.

Figure 1.3. The two pathways of apoptosis.

Figure 1.4. Structural analysis of the binding interface between Smac/Diablo and the BIR3 domain of XIAP.

Figure 1.5. Water-soluble CdSe/ZnS QDs functionalised with a targeting moiety.

Figure 2.1. General setup for the organometallic synthesis of CdSe/ZnS core-shell QDs.

Figure 2.2. PL spectra of CdSe core and CdSe/ZnS core-shell QDs.

Figure 2.3. High resolution-TEM micrograph of CdSe/ZnS core-shell QDs.

Figure 2.4. EDS spectrum of the as prepared CdSe/ZnS core-shell QDs.

Figure 2.5. Ligand exchange using L-cysteine.

Figure 3.1. Dose response curve of the Qdot525 (A) and Cys-QDs (B).

Figure 3.2. Schematic diagram illustrating cross-linking of the Qdot525 or Cys-QDs with p.L and Smac.

Figure 3.3. Desalted QD peptide bi-conjugates.

Figure 3.4. Evaluating the cytotoxicity of the targeted drug delivery system.

Figure 3.5. Binding of the Qdot525 peptide bi-conjugates.

Figure 3.6. Binding of the Cys-QD peptide bi-conjugates.

Figure 3.7. Internalisation the Qdot525 peptide bi-conjugates.

Figure 3.8. Internalisation the Cys-QD peptide bi-conjugates.

LIST OF TABLES

Table 1.1. Cancer specific peptides identified by phage display libraries.

Table 1.2. Nanoparticle-based delivery systems.

Table 2.1. Bi-conjugation of the Qdot525 to p.L and Smac.

Table 2.2. Bi-conjugation of the Cys-QDs to p.L and Smac.



ABBREVIATIONS

AIF	: Apoptosis Inducing Factor
Bax	: Bcl-2-associated X protein
Bcl-2	: B-cell lymphoma 2
BIR	: Baculoviral IAP Repeat
Caspase	: Cysteine Aspartic Acid-Specific Protease
CdSe/ZnS	: Cadmium Selenide Zinc Sulphide
Cys	: Cysteine
DISC	: Death Inducing Signalling Complex
EDC	: 1-Ethyl-3-(3-Dimethylaminopropyl) Carbodiimide
EGFR	: Epidermal Growth Factor Receptor
EPR	: Enhanced Permeability and Retention
ErbB-2	: Epidermal Growth Factor Receptor Type 2
HR-TEM	: High Resolution Transmission Electron Microscopy
IAPs	: Inhibitor of Apoptosis Proteins
mAb	: Monoclonal Antibody
MTS	: Mitochondrial-Targeting Sequence
p.L	: LTVSPWY Peptide
QDs	: Quantum Dots



Smac/DIABLO: Second mitochondria-derived activator of caspases/ Direct AIP binding
protein with low PI

XIAP : X-linked Inhibitor of Apoptosis Protein



DEDICATION

For my family...



I can do all things through Christ who strengthens me. – Philippians 4:13

ACKNOWLEDGEMENTS

Lord, how amazing & gracious you are to me! Your strength carried me through this degree. I cannot express enough gratitude towards You. Thank You.

To my family, oh wow. *My support*. This achievement wouldn't be worth having if I didn't have anyone to share it with. You've shared in my frustrations, my joy, my explanations that left you disliking science (laughing), for a moment, and then liking it again... for my sake of course! I love you all dearly. I'd like to give a special thanks to my sisters, Rochelle and Michaela, for helping me type this thesis when I was ill. I appreciate it!!!

Dr Mervin Meyer, my supervisor. Simply put, he's the best. Thank you for being my forerunner and helper, at the same time. Your time invested, it doesn't go unnoticed. To my co-supervisor, Dr Martin Onani, thank you for believing in me, your encouraging words and proofreading my thesis. To Dr Paul Mushonga, what a tremendous help! You brought out the '*chemist in me*'. Thank you for diligently teaching me – on that special *white board* ☺. Thank you to the Organometallic laboratory, what a lovely bunch! So welcoming and very helpful. To all my colleagues in the Biotechnology department, thank you. The laughs, the talks and the motivation. A special thank you to Bridget Daniels, one of the most helpful people I know.

I would also like to express my sincere gratitude to Valencia Jamalie and Chyril Abrahams. Your support is invaluable. Also, thank you Ayorinde James, your friendship, motivation and insight during the last few months of my project helped me to persevere. Thank you very much to my Mount Hope church family for your prayers and encouragements.

Thank you to the National Nanoscience Teaching and training Platform and Department of Science and Technology for funding this project.

Chapter One: Literature Review

1.1. Introduction

Mortality tolls presented by cancer are staggering in spite of progressive efforts in development of cancer therapies. Globally, annual projections are said to reach approximately 16 million new cases by 2020 (Thundimadathil, 2012). Inadequate capabilities to direct therapeutic moieties to a specific target site, through minimal interaction with healthy cells, largely account for the lack in translating research into clinical practice (Ferrari, 2005). Since cancer cells are characterised by their ability to proliferate autonomously and with time acquire multiple mutations, multidrug resistance is instigated. Consequently, current drug treatments are attesting to be less effective and there is therefore an urgency to develop improved cancer treatment options (Sumer and Gao, 2008 & Sioud and Mobergslie, 2012). Nanoparticle delivery systems offer an improved alternative due to their ability to interact at the cellular level with a great degree of specificity (Byrne *et al.*, 2008 & Singh and Lilard, 2009). To efficiently execute this, a better understanding of cancer growth, structure and physiology is required (Steichen *et al.*, 2012).

1.2. Cancer development

1.2.1. Tumour physiology

Cancer may be described as the abnormal growth of cells. Customarily, when a cell recognises any sort of impairment to its DNA, repair mechanisms are initiated. However, failure to execute this gives rise to genomic instabilities; consequently a cancerous cell is formed (Gotter 2009). In the advent of maintaining normal biological processes, cancerous cells along with healthy cells grow and divide to form new cells, but normal systematic processes often eliminate these cells through programmed cell death/apoptosis. However,

cancer cells can acquire mutations resulting in malfunctioned apoptotic signalling and in turn the cells escape apoptosis, multiplying unhindered to form tumour masses (Figure 1.1). Of note, is that the replication rates of cancerous cells outcompete that of healthy cells and in so doing, prompt a higher demand for nutrient supply; consequently, displacing healthy cells (Brannon-Peppers and Blanchette, 2004 & Steichen *et al.*, 2012). Initial tumour growth stages rely on diffusion of nutrients restricting tumour size limit to approximately 2 mm^3 . To overcome this diffusion limit, the tumour is required to recruit new blood vessels; and this is accomplished through a process called angiogenesis (Danhier *et al.*, 2010 & Steichen *et al.*, 2012).

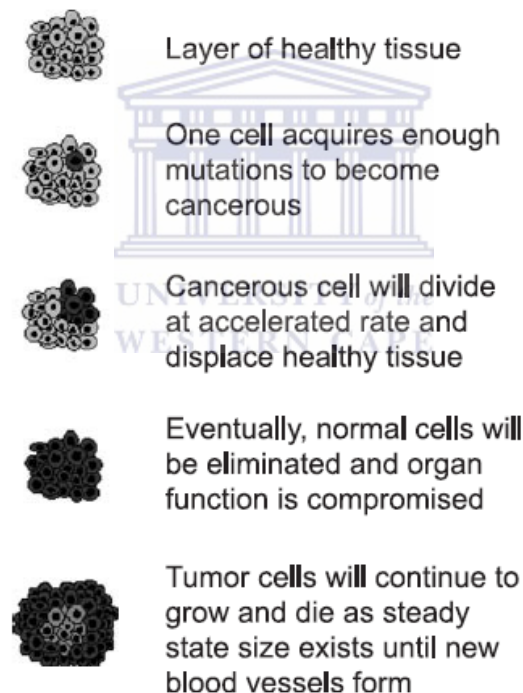


Figure 1.1. Tumour growth from a single cell. A single cancerous cell around healthy tissue undergoes replication at a much higher rate than normal cells and in so doing, displaces healthy tissue and eventually forming a tumour mass (Adapted from Brannon-Peppers and Blanchette, 2004).

1.2.2. Tumour vasculature

Angiogenesis comprises the construction of new blood vessels from pre-existing vessels and once the tumour reaches its solid size state (2 mm^3), hypoxia is initiated; subsequently

inducing angiogenesis (Danhier *et al.*, 2010). More importantly, the number of endothelial cells usually exist in a relatively dormant state, with about 1 in every 10 000 endothelial cells subjected to cell division. During angiogenesis, however, the turn-over increases up to 50 times (Brannon-Peppers and Blanchette, 2004). Since an adequate blood supply is absolutely necessary for tumour growth, blood vessels then rapidly grow, generating a highly disorganised and irregular vasculature with some regions rich in blood supply and others low in blood supply (Brannon-Peppers and Blanchette, 2004 & Byrne *et al.*, 2008 & Danhier *et al.*, 2010). Discrepancies in the vasculature lead to significantly varied degrees of blood flow throughout the tumour (Brannon-Peppers and Blanchette, 2004). Furthermore, poor vasculature results in generation of dead-ended vessels as a result of incomplete endothelial linings, essentially instigating leaky and highly permeable tumour vessels that easily allow macromolecules into the tumour interstitium (Steichen *et al.*, 2012 & Yu *et al.*, 2012). The combination of the aforementioned factors results in a condition known as the enhanced permeability and retention effect (EPR) which is a phenomenon exploited for delivery of conventional anti-cancer drugs (Steichen *et al.*, 2013).

1.3. Challenges in current cancer therapeutics

Conventional chemotherapy, was regarded as the most effective and preferred method of treatment owing to its extensive success in the killing of rapidly dividing cancer cells. However, restricted drug dosage, adverse side effects and systematic toxicities remains a concern, since rapidly growing healthy cells are also affected by the non-specific distribution of the cytotoxic drugs administered (Wang *et al.*, 2009 & Nguyen, 2011 & Sioud and Mobergslien, 2012). Furthermore, challenges presented by cells that have assimilated drug resistance; results in significantly poor responses to the chemotherapy. As a consequence, cancer cells can continue to proliferate uncontrolled; reassemble tumours and metastasize;

resulting in poor prognosis (Sumer and Gao, 2008). In view of this, the therapeutic goal of chemotherapy has shifted towards selective and proficient eradication of cancer cells whilst preserving healthy cells by using targeted drug delivery systems (Haglund *et al.*, 2009 & Sioud and Mobergslie, 2012 & Thundimadathil, 2012).

1.4. Targeted drug delivery systems

To effectively eliminate cancerous cells with increased efficacy, three essential dynamics should be considered; firstly, enhanced selectivity towards the target, secondly, therapeutic moieties should be designed in such a way that they are capable of bypassing biological barriers and lastly, the therapeutic agent should be capable of selectively killing cancerous cells once it reaches the target site (Ferrari, 2005 & Co *et al.*, 2008). Delivery of therapeutic agents to the target site may be accomplished by two modes of action, that is, passive or active targeting (Ferrari, 2005 & Wang *et al.*, 2008).

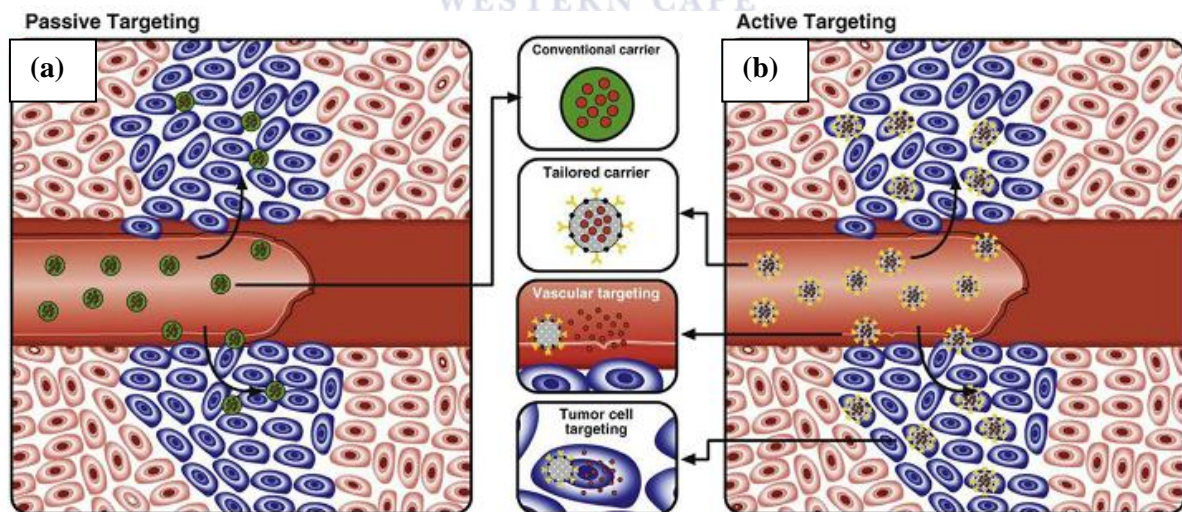


Figure 1.2. Passive versus active targeting. (a) Passive targeting relies on leaky blood vessels for diffusion of particles to the tumour site, whereas; (b) active targeting relies on the targeting moiety to deliver the particles directly to the tumour site (Adapted from de Barros *et al.*, 2012).

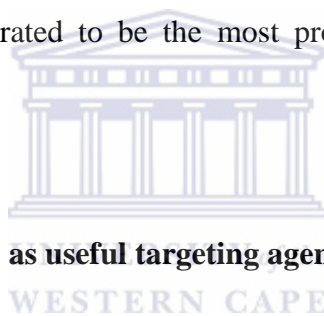
1.4.1. Passive targeting

Passive targeting is best described as the selective accumulation of drugs or drug delivery systems at the tumour site. This approach allows the exploitation of pathophysiological opportunities by means of the EPR effect (Vasir *et al.*, 2005; Cho *et al.*, 2008 & Danhier *et al.*, 2010). Since cancerous tissues are characterised by defective blood vessels and deficient lymph vessels, the targeted drug delivery system permeabilises the tissue with great ease (Vasir *et al.*, 2005). In some cases, cancer cells overexpress enzymes that are essential for metastasis, for example, matrix metalloproteinases (MMPs) (Wang *et al.*, 2008). Based on this concept, Wang *et al.*, (2008) developed a tumour activated pro-drug treatment, in which a nanoparticle was attached to doxorubicin (DOX) through albumin and an MMP-2 specific peptide. Upon successful cellular uptake, the conjugated MMP-2 specific peptide was cleaved by intracellular MMP-2, rendering the DOX activated and therefore able to exert anti-cancer activity (Wang *et al.*, 2008). Although passive targeting appears efficient, specificity remains a challenge. Furthermore, the use of the EPR effect may not be a practicable approach in all tumour types; since the degree of cell membrane penetrability differs between tumour type and stage. To overcome this limitation, the use of a targeting ligand as an amended alternative had been applied (Cho *et al.*, 2008).

1.4.2. Active targeting

Active targeting relies on the generation of a ternary structure consisting of a drug carrier, an active chemotherapeutic drug and a targeting moiety capable of binding to surface proteins of cancerous cells that are either uniquely expressed or overexpressed in cancer cells as compared to normal cells (Cho *et al.*, 2008 & Danhier *et al.*, 2010). An example of this nature is the use of monoclonal antibodies (mAb's) bi-conjugated to an anti-cancer drug, known as, Gefitinib (Abou-Jawde *et al.*, 2003). This FDA approved targeted cancer treatment exerts its

effect by blocking epidermal growth factor receptors and tyrosine kinase activity for advanced non-small cell lung cancer (Brannon-Peppers and Blanchette, 2004). However, the use of mAb's presents a number of challenges, one of which restricts their *in vivo* application, since repeated administration may induce an immune response that may in turn promptly clear the immunoconjugates from the bloodstream (Vasir *et al.*, 2005). Alternative strategies to circumvent current limitations using antibodies are under way, but taking this limitation into account, the targeting moiety is particularly important for cellular internalisation and effective transportation of the drug to the tumour site (Figure 1.2) (Byrne *et al.*, 2008). Therefore, in the advent of establishing efficient delivery of therapeutic agents into cancerous cells, various delivery agents have been explored for targeted delivery; of which cancer targeting peptides have demonstrated to be the most promising non-immunogenic agents (Shadidi and Sioud, 2003).



1.5. Cancer specific peptides as useful targeting agents

1.5.1. Why peptides?

The most popular molecular targeting agents used in the past, were mAb's, however, mAb's are extensively limited by non-specific localisation due to low internalisation efficacy as a result of high molecular weight (Shadidi and Sioud, 2003 & Li and Cho, 2011) and uptake by the mononuclear phagocyte system (Li and Cho, 2011). The cellular digestion process serves to break down any potential pathogens prior to accessing the cell. During endocytosis, a small part of the cells' outer membrane gets pinched off within the cell, forming a vesicle containing the potentially pathogenic material. These vesicles then fuse with intrinsic degradative material which determines the fate of the endocytosed material (Nichols and Bae, 2012). In this respect, the application of small peptides as an alternative targeting agent emerged to circumvent limitations presented by mAb's (Shadidi and Sioud, 2003).

Advantages demonstrated by peptide-based targeting include the generation of high-affinity sequences that are easy to generate using combinatorial screening and easy to conjugate to their counterparts (Jaracz *et al.*, 2005). The small size of peptides, usually less than 50 amino acids in length, permits a good degree of tissue penetrability, therefore highlighting them as ideal drug carriers to the tumour site (Shadidi and Sioud, 2003 & Li and Cho, 2012). Additionally, small peptides as targeting agents have demonstrated a considerable level of *in vivo* stability (Jaracz *et al.*, 2005 & Li and Cho, 2012) and contrary to mAb's, peptides are virtually undetectable by the immune system and are therefore expected to induce minimal, if any, side effects (Shadidi and Sioud, 2003).

1.5.2. Development of targeting peptides against cancer gene expression patterns

Genetically, cancer cells uniquely express a distinguishable pattern of genes as compared to healthy cells. This has been validated by high throughput technologies used to determine cancer type gene expression configurations. Subsequently, this has led to the discovery of very promising biomarkers for cancer-type specific targeting (Shadidi and Sioud, 2003). These biomarkers include cellular surface proteins, some having the ability to interact with the cancer specific peptides in a drug delivery system and subsequently subjected to receptor mediated endocytosis, and in so doing create a platform for drug delivery (Svensen *et al.*, 2012).

1.5.3. The identification of targeting peptides

Cancer specific peptides have been identified using phage display peptide libraries (Sioud and Mobergslien, 2012 & Svensen *et al.*, 2012). This approach involves screening virtually all possible short peptide sequences against identified cell surface proteins or cancer cells. Table 1.1 lists some cancer specific peptides identified by this technique.

Table 1.1. Cancer specific peptides identified by phage display libraries

Peptide ligand	Peptide sequence	Cellular target	Reference
Surface immunoglobulin	IELLQAR	E-Selectin	Fukuda <i>et al.</i> , 2000
Cancer cell surface	KCCYSL	Her-2 tyrosine kinase type 1 receptor	Karasseva <i>et al.</i> , 2002
	LTVSPWY	Human breast cancer cells	Shadidi and Sioud, 2003
	CVFXXXYXXC	Prostate specific antigen	Wu <i>et al.</i> , 2000
Vasculature	CTTHWGFTLC	MMP-2 and MMP-9	Koivunen <i>et al.</i> , 1999

Often, the selection of cancer specific peptides is based on their interaction with cell surface proteins involved in biological functions, for example, the family of epidermal growth factor receptors (EGFR) which is known to be overexpressed in a number of tumour types (Shadidi and Sioud, 2003 & Steichen *et al.*, 2013). The epidermal growth factor receptor type 2 (erbB-2) tyrosine kinase is a receptor whose biological functions are implicated in tumour cell survival, proliferation and metastases. The most emphasised area of concern with erbB-2 overexpression is associated with activation of downstream signalling pathways that promote cell survival (Wang *et al.*, 2005). One such example is Akt, a serine/threonine kinase (Kim *et al.*, 2005 & Wang *et al.*, 2005 & Normanno *et al.*, 2006) which upon activation, exerts its anti-apoptotic effects by phosphorylating two kinds of targets, (1) apoptosis regulatory proteins, such as caspase 9 and/or (2) substrates that indirectly inhibit apoptosis (Wang *et al.*, 2005). Furthermore, erbB-2's overexpression and activation has been shown to induce drug resistance and serve as a poor prognostic marker. Cancer specific peptides that are able to

bind erbB-2, can block signalling through this pathway, thus providing a promising avenue in cancer therapy since its overexpression has been observed in approximately 30% of breast cancer cell lines and is associated with poor prognosis in ovarian, colon and bladder cancers (Shadidi and Sioud, 2003 & Xu *et al.*, 2005). Markedly, non-peptide small EGFR/erbB-2 molecule inhibitors have advanced to clinical trials, however, with a low degree of success. Alternative potent inhibitors of EGFR/erbB-2 are therefore required. In this respect, a cancer specific peptide presents itself as an ideal possibility (Xu *et al.*, 2005).

1.5.4. The LTVSPWY peptide

LTVPSWY (denoted as p.L), a heptapeptide identified by Shadidi and Sioud (2002) has been shown to target and inhibit erbB-2 gene expression by selective delivery of an antisense phosphorothioate oligonucleotide to erbB-2 positive tumour cells (Shadidi and Sioud, 2002). It was then demonstrated that the p.L peptide bi-conjugated to the pro-apoptotic α -tocopheryl succinate (α -TOS) induced a significantly higher degree of apoptosis in erbB-2 positive breast cancer cells than untargeted α -TOS (Wang *et al.*, 2007). In another study, the p.L peptide was used to deliver the pro-apoptotic peptide (KLAKLAK)₂ to breast cancer cells and selectively kill them (Sioud and Mobergslien, 2012). Furthermore, the p.L peptide has been shown to be internalised by SKBR3 (Shadidi and Sioud, 2002), MDA-MB-453, MDA-MB-231 and MC7 breast cancer cells (Sioud and Mobergslien, 2012) as well as SKOV-3 human ovarian carcinoma cells (Jie *et al.*, 2012). Since the p.L peptide facilitates targeting and internalisation in a number of cancer cell lines, it has emerged as a favourable candidate for peptide-directed delivery of therapeutic agents to erbB-2 expressing cell lines (Wang *et al.*, 2007 & Haglund *et al.*, 2009 & Jie *et al.*, 2012 & Sioud and Mobergslien, 2012).

1.6. Cancer and apoptosis

1.6.1. The role of apoptosis in cancer progression

Cancer development and progression is allied to abnormalities in biochemical pathways (Fry and Vassiley, 2005). ErbB-2 overexpression in cancer cells is associated with one of these pathways, namely, the apoptotic signalling pathway (Wang *et al.*, 2005). Apoptosis may be defined as a highly regulated form of cell death (Wang *et al.*, 2005 & Kroemer *et al.*, 2005 & Rastogi *et al.*, 2009). Apoptotic cells are characterised by morphological changes such as cell shrinkage, chromatin condensation and DNA fragmentation and subsequent removal by phagocytosis (Narula *et al.*, 1996 & Gewies 2003).

The fundamentals of apoptosis are characterised and executed by cysteine aspartic acid-specific proteases (or Caspases) (Fulda and Debatin, 2006) which are synthesised as pro-enzymes and generally occur in cells in an inactive form, i.e. as a pro-caspase. Upon activation, caspases cleave several substrates, activate other pro-caspases; and in doing so, stimulate the protease cascade by magnifying apoptosis signalling ultimately leading to cell death (Rastogi *et al.*, 2009). Caspases are characterised based on their role in the apoptotic pathway, i.e. initiator caspases (which initiate disassembly in response to apoptotic stimuli, e.g. caspase 2, 8, 9 and 10) or effector caspases (which has direct function in disassembly of cells, e.g. caspase 3, 6 and 7) (Gill *et al.*, 2006 & Rastogi *et al.*, 2009). Caspase activation occurs in response to one of two well defined apoptotic pathways, i.e. the extrinsic pathway or the intrinsic pathway as seen in Figure 1.3 (Fulda and Debatin, 2006).

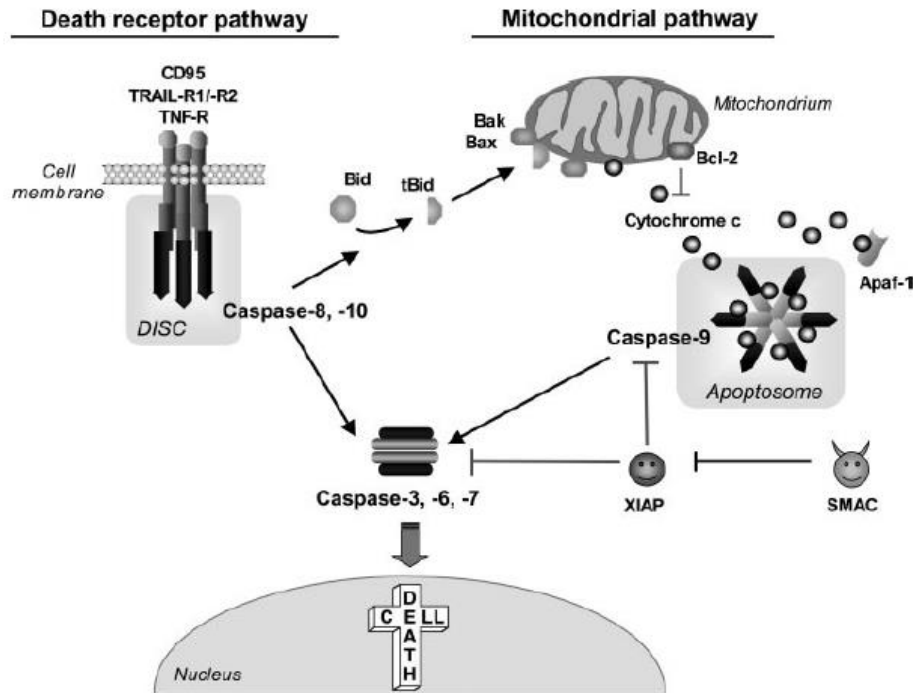


Figure 1.3. The two pathways of apoptosis. The death receptor pathway is facilitated by death receptors that recruit death domain adaptor molecules to form a death inducing signalling complex to activate caspase 8/10 and in turn downstream caspases. However, the mitochondrial pathway is initiated in response to cellular stress. Subsequently, pro-apoptotic proteins are released from the mitochondria and activate caspase 9 and in turn downstream caspases (Fischer and Schulze-Osthoff, 2005).

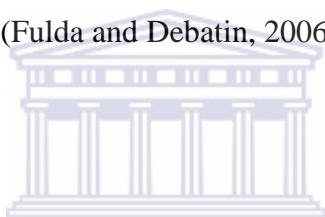
1.6.2. Apoptosis pathways

1.6.2.1. The Extrinsic pathway

The extrinsic pathway is initiated by means of death receptor signalling, across the cell membrane, in which the death receptors bind a ligand. Subsequent recruitment of death domain adaptor molecules occurs, leading up to formation of a death inducing signalling complex (DISC) which in turn activates pro-caspase 8/10 and eventually resulting in cell death or activation of the intrinsic pathway (Scaffidi *et al.*, 1998 & Gill *et al.*, 2006 & Fulda and Debatin, 2006 & Rastogi *et al.*, 2009).

1.6.2.2. The Intrinsic pathway

The intrinsic pathway is initiated and regulated by the mitochondria (Gill *et al.*, 2006). This pathway is prompted by various cytotoxic stimuli such as DNA damage, defects in the cell-cycle check point and loss of survival factors which ultimately lead to mitochondrial damage (Wang and El-Deiry, 2003 & Gill *et al.*, 2006). Consequently, B-cell lymphoma 2 associated X protein (Bax) expression is upregulated and/or B-cell lymphoma 2 (Bcl-2) expression is downregulated. The outer membrane of the mitochondria is then permeabilised, inducing the release of pro-apoptotic agents into the cytosol, i.e. cytochrome *c*, Second mitochondria-derived activator of caspases/ Direct AIP binding protein with low PI (Smac/DIABLO) and apoptosis inducing factor (AIF) which then promotes caspase activation and allows for execution of cell death (Figure 3) (Fulda and Debatin, 2006; Gill *et al.*, 2006 & Rastogi *et al.*, 2009 & Wang *et al.*, 2011).



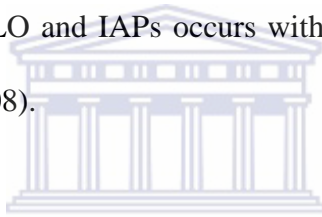
1.6.3. Pro-apoptotic agents as anti-cancer drugs

In light of the aberrant regulatory apoptotic signalling pathways, numerous components along the pathways elicit a targeting prospect which would facilitate the treatment of cancer. From the aforementioned, overexpression of erbB-2 as an example and other cancer cell surface receptors alike would provide a preparatory phase in an active targeted drug delivery system (Wang *et al.*, 2005). Additionally, designing agents that are able to exert inhibitory effects on anti-apoptotic proteins, such as, IAPs in cancer cells provides the second phase of targeting, in that it could enhance the efficiency of current chemotherapeutic drugs at lower dosages (Arnt and Kaufmann, 2003 & Wang *et al.*, 2005).

1.7. Smac/DIABLO: a pro-apoptotic agent

1.7.1. Smac/DIABLO

Smac/DIABLO is a pro-apoptotic protein secreted from mitochondria in response to several apoptogenic signalling (Martinez-Ruiz *et al.*, 2008). The wild-type Smac/DIABLO protein is 239 amino acids in length upon synthesis in the mitochondria; with the first 55 amino acids of the NH₂-terminal identified as the mitochondrial-targeting sequence (MTS) (Chai *et al.*, 2000 & Wu *et al.*, 2000 & Shiozaki and Shi, 2004). In the event of apoptotic stimuli, the MTS is cleaved by post-translational modifications and subsequently a tetrapeptide motif (Ala-Val-Pro-Ile) is exposed to allow interaction between Smac/DIABLO and IAPs (Wu *et al.*, 2000 & Gao *et al.*, 2007 & Martinez-Ruiz *et al.*, 2008). Several studies have demonstrated that the interaction between Smac/DIABLO and IAPs occurs with the baculoviral IAP repeat (BIR) domain (Martinez-Ruiz *et al.*, 2008).



1.7.2. Smac/DIABLO association with Inhibitors of apoptosis proteins

The IAP family of proteins is characterised based on its apoptosis suppressor effect (Wilkinson *et al.*, 2004) rendered by their BIR domain (Deveraux and Reed, 1999 and Arnt *et al.*, 2002). A total of three tandem copies (BIR1, BIR2 and BIR3) of this domain may occur within the IAP proteins (Deveraux and Reed, 1999). The IAP family of proteins comprises of eight human analogues of which X-linked IAP (XIAP), cellular IAP1 (cIAP1) and cIAP2 show the greatest degree of structural homology (Arnt *et al.*, 2002) and are well characterised as having direct caspase inhibitory activity (Deveraux and Reed, 1999; Wilkinson *et al.*, 2004 & Fulda, 2009). Furthermore, it has been shown that increased expression of XIAP induces a protective effect against apoptosis in cancer cells (Holcik *et al.*, 2003). This inhibitory effect is exerted by binding of the BIR domain to target caspases in such a way that upstream amino acids of the caspase active site are eclipsed; consequently preventing caspase activation (Wei

et al., 2008). This in turn prompts the degradation of the caspases by the proteasome, thereby, inhibiting apoptosis (Martinez-Ruiz *et al.*, 2008). It is important to note that in mammalian systems, different IAPs exert their anti-apoptotic effects on caspases, differently. For example, IAPs may compete with the apoptosis protease activating factor 1 for binding to pro-caspase 9, thus obstructing the formation of the apoptosome (Wei *et al.*, 2008). However, Smac/DIABLO release from the mitochondria in response to apoptotic stimuli takes on an IAP antagonistic role by disrupting interaction between IAP's and the corresponding caspases (Arnt and Kaufmann, 2003). Structural analysis (Figure 1.4) has demonstrated that Smac/DIABLO associates with IAP's at the BIR3 domain of XIAP by means of its' N-terminal AVPI motif (Wu *et al.*, 2000).

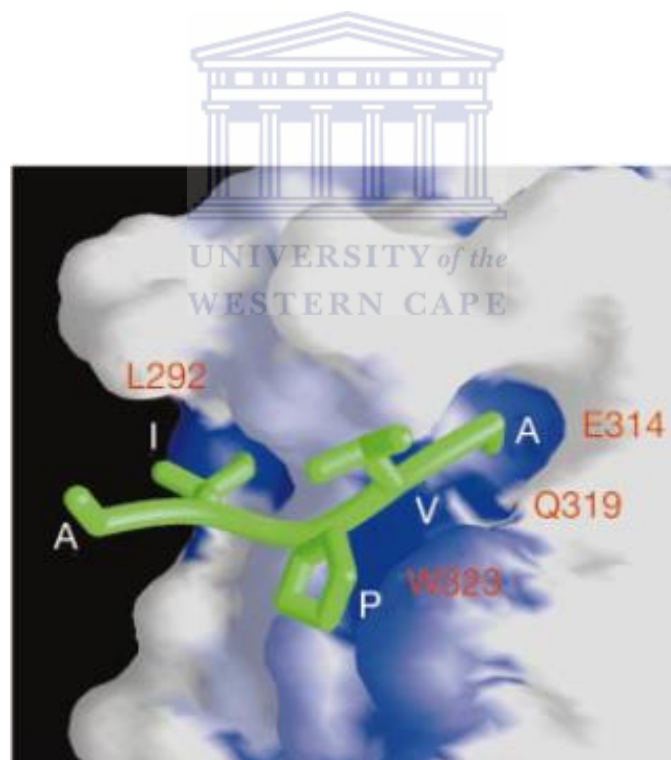


Figure 1.4. Structural analysis of the binding interface between Smac/DIABLO and the BIR3 domain of XIAP. The first 4 amino acids of Smac/DIABLO's N-terminus fits into the binding groove of XIAP's BIR3 domain. The blue and white regions signify greatest and slightest hydrophobic surfaces, respectively and the N-terminal of Smac is depicted in green. (Adapted from Wu *et al.*, 2000).

XIAP has three BIR domains and is regarded as the most powerful endogenous IAP, having very high affinity to caspases (Wei *et al.*, 2008). The BIR2 and BIR3 domains display specific binding and inhibitory properties against caspase 3 and 7 (Takeuchi *et al.*, 2005 & Tamm *et al.*, 2007). In the case of caspase 9 inhibition, it has been shown that BIR3 and RING domains are required (Deveraux and Reed, 2000). Usually, the BIR3 domain would form a heterodimer with the monomeric and active form of caspase 9; however, no physical binding to caspase 9 active site occurs (Wei *et al.*, 2008). This results in the prevention of caspase 9 dimerization and also holds it in an inactive structural conformation, thereby, inhibiting downstream apoptotic signalling (Shiozaki and Shi, 2004 & Wei *et al.*, 2008). Caspase 9 possesses an IAP binding tetrapeptide motif, Ala-Thr-Pro-Phe (Srinivasula *et al.*, 2001). If pro-caspase 9 is not proteolytically processed, it is unable to stably complex with IAPs, however, in the reverse scenario; this motif is exposed and becomes easily accessible for interaction with XIAP (Shiozaki and Shi, 2004). In the event of apoptosis, the mature form of Smac/DIABLO released from the mitochondria uses a similar tetrapeptide motif (Ala-Val-Pro-Ile) to competitively bind XIAP, and thus interfere with the XIAP-caspase 9 complex and exert a pro-apoptotic effect (Shiozaki and Shi, 2004 & Wu *et al.*, 2008). Based on this interaction, Smac/DIABLO agonists are considered to be co-anti-cancer therapeutic agents augmenting well-defined chemotherapeutic drugs (Arnt *et al.*, 2002 & Fandy *et al.*, 2008).

1.7.3. The application of Smac/DIABLO in the treatment of cancer

Smac/DIABLO as well as Smac-derived short peptides have been demonstrated to enhance the anti-cancer activity of some drugs that induce apoptosis in cancer cells (Chai *et al.*, 2000 & Arnt and Kaufmann, 2003 & Martinez-Ruiz *et al.*, 2008 & Lu *et al.*, 2011). Several studies have been carried out to demonstrate the sensitisation of cancer cells to a panel of pro-

apoptotic drugs in the presence of overexpressed Smac/DIABLO and/or its peptide derivatives (Martinez-Ruiz *et al.*, 2008). One such example, according to Arnt *et al.*, 2002, is Smac/DIABLO. The first 4-8 N-terminal amino acids of Smac/DIABLO was conjugated to the penetratin sequence (a carrier peptide that is able to permeabilise the cell membrane) and as a result enhanced the degree of apoptosis as well as the long term anti-proliferative effects induced by a variety of antineoplastic agents in MCF7 cells. Furthermore, *in situ* analysis revealed that this fusion peptide bound XIAP and cIAP1, subsequently displaces caspase-3 aggregates; and in so doing enhance the drug-induced caspase activity (Arnt *et al.*, 2002).

Another study demonstrated that the first seven amino acids of the N-terminus of Smac/DIABLO sensitised *in vivo* models of an intracranial malignant glioma xenograft to the anti-tumour activity of the tumour necrosis factor- α -related apoptosis-inducing ligand (TRAIL) (Fandy *et al.*, 2008). More importantly, only co-treatment of TRAIL and Smac/DIABLO peptides completely eliminated tumours and resulted in survival of mice with no detectable toxicity. Interestingly, N-terminal Smac/DIABLO peptides only sensitise low expressing IAP tumour cells to apoptosis, but are able to induce apoptosis in high expressing IAP tumour cells. This reveals that the level of IAP expression in various tumour types determines how different tumours will respond to these peptides; and thus, the prospective effect of Smac/DIABLO (Fandy *et al.*, 2008). This treatment strategy has the potential to reduce anti-cancer dosages whilst increasing intra-cellular concentrations, thereby improving patient survival rates (Cho *et al.*, 2008).

In a study conducted by Guo *et al.*, co-treatment of the N-terminal heptapeptide (Smac-7) and tetrapeptide (Smac-4) of Smac/DIABLO with either epothilone (Epo) B derivative BMS 247550 (an antimicrotubule agent) or TRAIL significantly increased the level of apoptosis,

observed by PARP cleavage activity exerted on caspase 3. It was also observed that increased levels of apoptosis was directly associated with down-regulation of XIAP, cIAP and survivin. It was concluded that co-treatment with N-terminal Smac/DIABLO peptides effectively enhances the apoptosis signalling and may improve anti-tumour activity of Epo B and TRAIL (Guo *et al.*, 2002).

1.8. Nanotechnology-based drug delivery systems

1.8.1. Nanotechnology

Taking into account the therapeutic goal of anti-cancer treatment is the selective eradication of cancer cells; most conventional anti-cancer drug treatments are ineffective as a result of non-specific distribution of the drug (Sinha *et al.*, 2006). Therefore, alternative drug delivery methods are required. Nanotechnology has emerged as a promising strategy to develop appropriate and efficient drug carriers for targeted drug delivery systems (Yu *et al.*, 2012). Nanotechnology is the field of science that relates to technological systems based on small sized materials, ranging between 1 - 100 nm. It is this size range that allows the exhibition of novel properties in nanomaterials, distinguishing them from bulk materials with respect to physical and chemical properties (Cao and Wang, 2011).

Nanoparticles have the ability to enter the smallest capillary vessels and circumvent rapid clearance by phagocytes (Cho *et al.*, 2008). Therefore, successfully prolonging their blood circulation time and increasing the chances as well as drug load reaching the target site (Cho *et al.*, 2008 & Nichols and Bae, 2012). Depending on the size and surface characteristics, unmodified nanoparticles are generally seized by the reticuloendothelial system (Cho *et al.*, 2008). Numerous nanoparticles have successfully been employed in the development of drug delivery systems for use in cancer therapy (Table 1.2) (Pal and Nayak, 2010).

Table 1.2. Nanoparticle-based delivery systems.

Nanoparticle-based delivery system	Therapeutic application
Liposomes	Controlled and targeted drug delivery Targeted gene delivery
Polymeric Micelles	Controlled and targeted drug delivery
Dendrimers	Targeted drug delivery
Gold nanoparticles	Targeted delivery and imaging agent
QDs	Targeting and imaging agent

Adapted from Pal and Nayak, 2010.

Nanomaterials may be categorised based on quantization effects, i.e. when the charged carriers are confined in either one, two or three dimensions. For example, nano-structures confined in one dimension, are categorised as two dimensional structures; however, if they are confined in two dimensions, they are considered as a one dimensional structure and lastly, if confined in three dimensions, they are regarded as zero dimensional structures, which is the category into which QDs are defined (Drbohlavova *et al.*, 2009).

1.8.2. QDs

1.8.2.1. Optical properties

QDs are semiconducting colloidal crystalline nanoparticles (Galian and Guardia, 2008). Their diameters generally range from 2 - 10 nm in size (Drbohlavova *et al.*, 2009) and are characterised based on quantum confinement effects, which is described by the radius of the crystalline nanoparticle that approaches values lower than one of the magnitudes illustrated by the Bohr radius of electron, hole and exciton, respectively (Chan *et al.*, 1998). As a result of size and the corresponding quantum confinement effects, QDs possess unique properties as

compared to bulk materials although having the same chemical composition (Mattheakis *et al.*, 2004).

With respect to semiconducting material, QDs exhibit useful optical properties which depend on the material used, the size of the particles, the size distribution and surface chemistry (Mattheakis *et al.*, 2004 & Resch-Genger *et al.*, 2008). These properties include the formation of broad absorption spectra which may be described as energy absorption of a photon above the semiconductor band gap resulting in formation of an exciton (Michalet *et al.*, 2005). Furthermore, radiative recombination of electron-hole pairs in QDs leads to a long fluorescence lifetime (20 – 50 ns) of photon emission as compared to conventional semiconductors (<10 ns) (Yoffe, 2001; Gao *et al.*, 2005 & Michalet *et al.*, 2005).



1.8.2.2. QDs versus organic fluorophores

QDs are widely used for cellular labelling and imaging of tissues and cells using fluorescence techniques (Resch-Genger *et al.*, 2008 & Medintz and Mattoussi, 2009). The optical properties mentioned above contribute significantly to the advantages offered by QDs as compared to conventional fluorophores (Michalet *et al.*, 2005 & Medintz and Mattoussi, 2009). QDs possess particular photo-physical properties, in particular, high photostability which result in preference to conventional organic dyes (Galian and Guardia, 2009). QDs are generally synthesised from atoms in group II and IV (Reiss *et al.*, 2009). Further addition of an inorganic shell produces core/shell QDs that have greater quantum yields than the uncoated ones (Frasco and Chaniotakis, 2009). To be precise, in QDs, PL is high in the visible as well as the near infrared ranges. However, PL for organic dyes is only high in the visible range (Resch-Genger *et al.*, 2008). QDs have the ability to gradually increase

absorption leading to shorter wavelengths and narrower emission bands. This may be manipulated by changing the particle size (Jin *et al.*, 2008 & Galian and Guardia, 2009).

Variation of size and composition of QDs makes it possible for wavelengths to be tuned from blue to near infrared. That is, the emission wavelength may be blue shifted and red shifted by smaller and larger QDs, respectively. Organic dyes may only fluoresce at a particular wavelength it was designed for (Chan *et al.*, 2002). Furthermore, the increase in fluorescence lifetime in QD leads to greater sensitivity. As mentioned earlier, QDs have an advantage in relation to photostability; this is made possible as a result of surface passivation, in which photo-oxidation may almost be completely suppressed by the inorganic shell coating. This is an attractive property for imaging techniques that involves intense laser excitation sources especially for long-term imaging (Resch-Genger *et al.*, 2008). The exploration of many fundamental biological processes is dependent on the rapid, sensitive and reproducible detection of biomolecule interactions and fluorescence techniques are applicable in accomplishing these objectives. Since QDs have been shown to possess improved properties in comparison to conventional fluorophores, QDs have therefore taken preference in many biological applications (Resch-Genger *et al.*, 2008).

1.9. The application of QDs in targeted drug delivery systems

1.9.1. Water-soluble QDs

Most reliable synthesis methods make use of organic solvents for production of highly monodispersed and homogenous nanostructures, resulting in the materials requiring solubilisation for biological application (Vo-Dinh, 2007). There are two processes to achieve biocompatibility for QDs; (1) ligand exchange, which involves native surface ligands being substituted with a bi-functional ligand containing an anchoring moiety (e.g. thiol) and a

hydrophilic functional group (e.g. $-\text{NH}_2$ or $-\text{COOH}$) and; (2) encapsulation of the native capping layer using amphilic polymers or silica (Zhang and Clapp, 2011). Once solubilised, QDs can be functionalised with biomolecules such as nucleic acids, carbohydrates, proteins, lipids and polymers and probed for target delivery, as shown in figure 1.5 (Vo-Dinh, 2007).

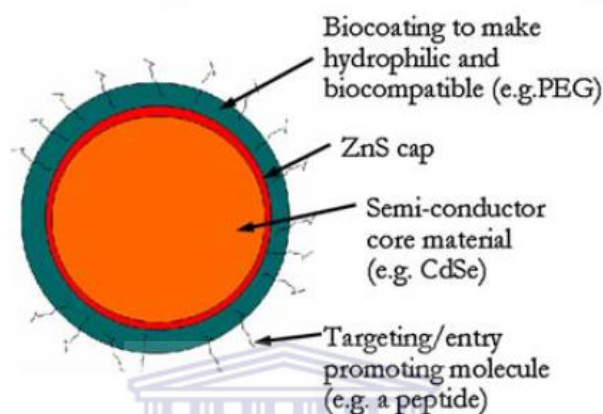


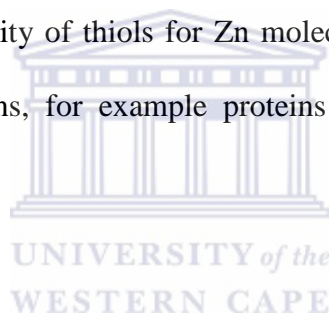
Figure 1.5. Water-soluble CdSe/ZnS QDs functionalised with a targeting moiety. (Adapted from Haglund *et al.*, 2009)

1.9.2. Bi-conjugation chemistry

In order to facilitate the use of a drug delivery system, the respective moieties are required to be chemically linked (Hermanson, 2013). This is achieved through the concept of bi-conjugation, which may be described as the covalent linkage of two or more molecules. Several bi-conjugation cross-linkers exist, therefore, choosing the appropriate one relies on the chemical groups available on the target molecules (Zhang and Clapp, 2011 & Hermanson, 2013).

Peptides have amino acids that are joined through the formation of covalent bonds. Each amino acid comprises of an amino group (N-terminal) and a carboxyl group (C-terminal)

(Hermanson, 2013). The N-terminal of peptides may be coupled to activated carboxylates, subsequently yielding amide bi-conjugates. Alternatively, the C-terminal may be exploited by bi-conjugation through formation of an amide bond (Hermanson, 2008). EDC is cross-linker most often employed to mediate the above described bi-conjugation. EDC is a zero-length cross-linker, that is, in the process of conjugation; no additional atoms are incorporated (Zhang and Clapp, 2011 & Vashist, 2012). This is advantageous, in that, the introduction of foreign structures by other cross-linkers may prompt interference in the function of the complexed biomolecule. EDC, therefore, excludes the susceptibility to any form of cross-reactivity by forming directly complexed bi-conjugates (Hermanson, 2008). Other methods of conjugation exist, such as the use of thiolated peptides which can directly attach to the ZnS coated QDs induced by the affinity of thiols for Zn molecules (Zhang and Clapp, 2011) or adsorption of engineered proteins, for example proteins with His-tags (Mattoussi *et al.*, 2000).



1.9.3. Peptide directed QDs

Work done by Haglund *et al.*, demonstrated the successful targeting to SkBR3 breast cancer cells using QDs bi-conjugated to the p.L peptide. This work illustrated the twofold functionality of the targeting peptide, that is, the QDs reaching the cell membrane and being internalised, as observed by the fluorescence of the QDs (Haglund *et al.*, 2009). Since the *in vitro* experiments showed success, the p.L peptide was then applied to an *in vivo* mouse model, having a human SkBR3 tumour xenograft. The QD/p.L peptide bi-conjugate was then injected into the tails of the mice and effectively targeted to the tumour mass (Haglund *et al.*, 2009).

In another study by Shi *et al.*, arginine-glycine-aspartic acid (RGD) peptides were bi-conjugated to QDs and used to target integrin $\alpha_v\beta_3$ which are crucial vehicles for metastatic

cancers (Felding-Habermann, 2000 & Shi *et al.*, 2006). The RGD motif was exploited for its high selectivity and affinity against integrin $\alpha_v\beta_3$. Also, important to note, integrin $\alpha_v\beta_3$ is known to be significantly upregulated in tumour tissues, but not in healthy tissue (Bentolila *et al.*, 2000). Using this model, several studies of *in vivo* tumour targeting and imaging were reported (Chen *et al.*, 2004 & Cai *et al.*, 2006 & Cai *et al.*, 2007).

1.9.4. Multifunctional QDs for cancer treatment

The multifunctional capacity of nanoparticles provides unique advantages for cancer diagnosis and treatments (Yu and Jon, 2012). The large surface area allows for functionalization of the nanoparticles with several ligands, that is, either retaining diagnostic or therapeutic properties (Haglund *et al.*, 2009 & Ho and Leong, 2010), presenting the QDs as a theranostic (diagnostic and therapeutic) modality (Ho and Leong, 2010).

A successful theranostic QD study presented by Bagalkot *et al.*, (2007), illustrates the conjugation of QDs to aptamers and DOX (QD-Apt-DOX). An RNA aptamer was designed to target and image prostate-specific membrane antigen (PSMA) expressed in LNCaP cells using the fluorescent properties offered by the QDs. The DOX moiety was intercalated within the aptamer and used in a fluorescence resonance energy transfer (FRET) based manner. In the drug-loading state, the fluorescence of both the QD and DOX were undetectable as a result of the aptamer that quenched the fluorescence of the DOX and subsequently DOX quenched the fluorescence of the QDs. However, in the drug-release state, DOX is released from the QD-Apt conjugate, resulting in the fluorescence of both DOX and the QDs. More importantly, the DOX fluorescence could be traced during transportation of the drug (Bagalkot *et al.*, 2007).

QDs have shown to be excellent imaging agents, for both *in vitro* and *in vivo* models. With the increasing application of QDs in therapeutic delivery, the potential use of QDs as a multifunctional modality is also increasing. However, there are still some controversies surrounding the potential cytotoxicity of QDs (Ho and Leong, 2010).

1.9.5. Cytotoxicity of QDs

QD toxicity is dependent on several factors, including, its size, composition and surface modifications (Winnik and Maysinger, 2013). Additionally, toxicity profiles may be attributed to inherent properties of the QDs as well as the environmental conditions (Hardman, 2006). Bhatia *et al.*, showed the relationship between cytotoxicity and the surface properties of QDs for an *in vitro* model. It was noted, that the oxidation of the QD surface prompted the reduced form of Cd, which in turn resulted in the release of free Cd ions. And the presence of Cd ions was strongly correlated to cell death (Bhatia *et al.*, 2004 & Chen *et al.*, 2011). Very important to note, each QD retains its own physicochemical properties and therefore, highlights the fact that all QDs are not alike, thus their physicochemical properties determine their potential cytotoxicity (Hardman, 2006). This was confirmed by several *in vitro* studies, illustrating that certain types of QDs may be toxic (Hoshino *et al.*, 2004 & Lovric *et al.*, 2005).

Most literature alludes to the fact that the dissipation of Cd leads to cytotoxic effects, however, chemically capping QDs with inert materials, for example, silica, serves as a good measure to avoid cellular toxicities (Gomes *et al.*, 2011).

1.10. Objective of this study

The objective of this study was to develop a multimodal nanoparticle-based targeted drug delivery system using peptide directed QDs as an imaging agent and delivery vehicle to selectively kill cancer cells using the pro-apoptotic peptide, Smac in combinatorial treatment with ceramide.



Chapter Two: The synthesis, characterisation and solubilisation of CdSe/ZnS core-shell QDs

2.1. Introduction

QDs are semiconductor colloidal crystalline nanoparticles with diameters, generally, ranging between 2 - 10 nm in size. They are characterised based on quantum confinement effects, resulting in QDs possessing unique optical properties as compared to bulk materials (Chan *et al.*, 1998 & Mattheakis *et al.*, 2004 & Galian and Guardia, 2008 & Drbohlavova *et al.*, 2009). In biological applications, fluorescent colloidal QDs have been reported to retain several advantages when compared to conventional organic fluorophores. These include, higher photostability, greater quantum yields; size and composition tunable wavelength emissions as well as increased fluorescence lifetimes (Chan *et al.*, 2002 & Michalet *et al.*, 2005 & Jin *et al.*, 2008 & Resch-Genger *et al.*, 2008 & Galian and Guardia, 2009 & Medintz and Mattoussi, 2009).

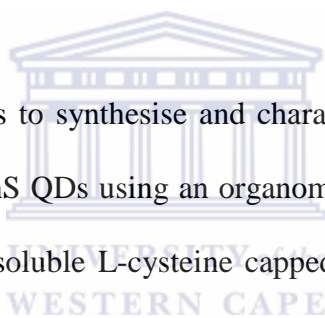
It is important to note that biological environments call for specific chemical and optical properties of nanoparticles applied to them. Since the photophysical properties of QDs are associated with its surface states, it is critical to direct the surface chemistry in such a way that biocompatibility, yet desirable optical properties and electronic passivation are retained in the aqueous medium (Jamieson *et al.*, 2007 & Zhang and Clapp, 2011). This has been a challenge, despite efforts to directly synthesise QDs using aqueous synthetic methods. It appears that most aqueous approaches produce moderately stable and low quantum yields. Consequently, an organometallic route remains a more reliable synthesis scheme (Zhang and Clapp, 2011).

Synthesis of highly monodispersed and highly fluorescent QDs is most commonly achieved at elevated temperatures, using organic solvents, such as trioctylphosphine (TOP) (Vo-Dinh,

2007 & Tiwari *et al.*, 2009). Even though QDs are generally synthesised from group II-VI atoms, CdSe/ZnS are most often employed in biological applications (Midentz *et al.*, 2005). The growth of QD core structure has been reported to occur in two stages, that is, step (1): nucleation which is then followed by step (2): Ostwald ripening, described as a mechanism in which small particles dissolve and deposit onto larger particles in solution to achieve a more thermodynamically stable state (Huy, *et al.*, 2011). To prevent CdSe oxidation or leakage and also attain high quantum yield, an inorganic material with a higher band gap is generally used, for example, ZnS (Dabbousi *et al.*, 1997).

2.2. Objective of this chapter

The objective of this chapter was to synthesise and characterise highly monodispersed and highly green fluorescent CdSe/ZnS QDs using an organometallic approach and to use the as prepared QDs to produce water-soluble L-cysteine capped CdSe/ZnS core-shell QDs to be applied in a biological application.



2.3. Materials and suppliers

1-Octadecene	Sigma-Aldrich
2-Propanol	Sigma-Aldrich
Acetone	Sigma-Aldrich
Argon	Afrox
Cadmium Oxide	Sigma-Aldrich
Ethanol	Merck
Hexane	Sigma-Aldrich
L-cysteine	Sigma-Aldrich
Liquid Nitrogen	Afrox
3-Mercaptopropionic acid	Sigma-Aldrich
Methanol	Merck
Phosphate buffered saline	Whitehead Scientific
Oleic acid	Sigma-Aldrich
Selenium powder	Sigma-Aldrich
Sodium Hydroxide	Merck
Sulfur	Sigma-Aldrich
Trioctylphosphine	Sigma-Aldrich
Zinc Undecylenate	Sigma-Aldrich



2.4. Methods

2.4.1. The organometallic synthesis of CdSe/ZnS core-shell QDs

Synthesis of the QDs was performed as described by Boatman and Lisensky, 2005 with minimal modifications. All reactions were setup under an inert atmosphere, created by careful purging of the system with nitrogen gas (**Figure 2.1**). All the flasks were sealed with rubber septa. A stock solution of the selenium (Se) precursor was prepared prior to synthesis, by addition of Se powder (0.2716 g) to 1-octadecene (ODE) (8 ml) and trioctylphosphine (TOP) (2 ml) in a two-necked flask. The mixture was heated in a silicon oil bath to 140 °C while stirring until dissolved to give a clear solution. Meanwhile, the cadmium-oleate precursor was synthesised by addition of cadmium oxide (0.110 g) to oleic acid (1 ml) in a three-necked flask. The mixture was then heated to 225 °C while stirring until complete dissolution of CdO with resultant formation of the Cd-oleate precursor. The temperature was then lowered to 120 °C and 2 ml of previously prepared Se precursor was rapidly injected into the Cd oleate mixture. At this point, the colour of the solution changed from clear to yellow. The nanoparticles were allowed to grow for 8 min. An aliquot (0.1 ml) was extracted at 8 min and dissolved in hexane. Subsequent quenching of the reaction was carried out by placing the solution on ice.

The CdSe core nanoparticles were then layered with a zinc sulphide (ZnS) shell. The sulphur (S) precursor was prepared by dissolution of S powder (0.138 g) in ODE (9 ml) and TOP (1 ml) at 140 °C, while stirring. This mixture was then allowed to cool down to room temperature. The Zn-TOP precursor was prepared by addition of zinc undecylate powder (1.857 g) to ODE and TOP. The Zn-TOP mixture was heated to 140 °C while stirring until complete dissolution.

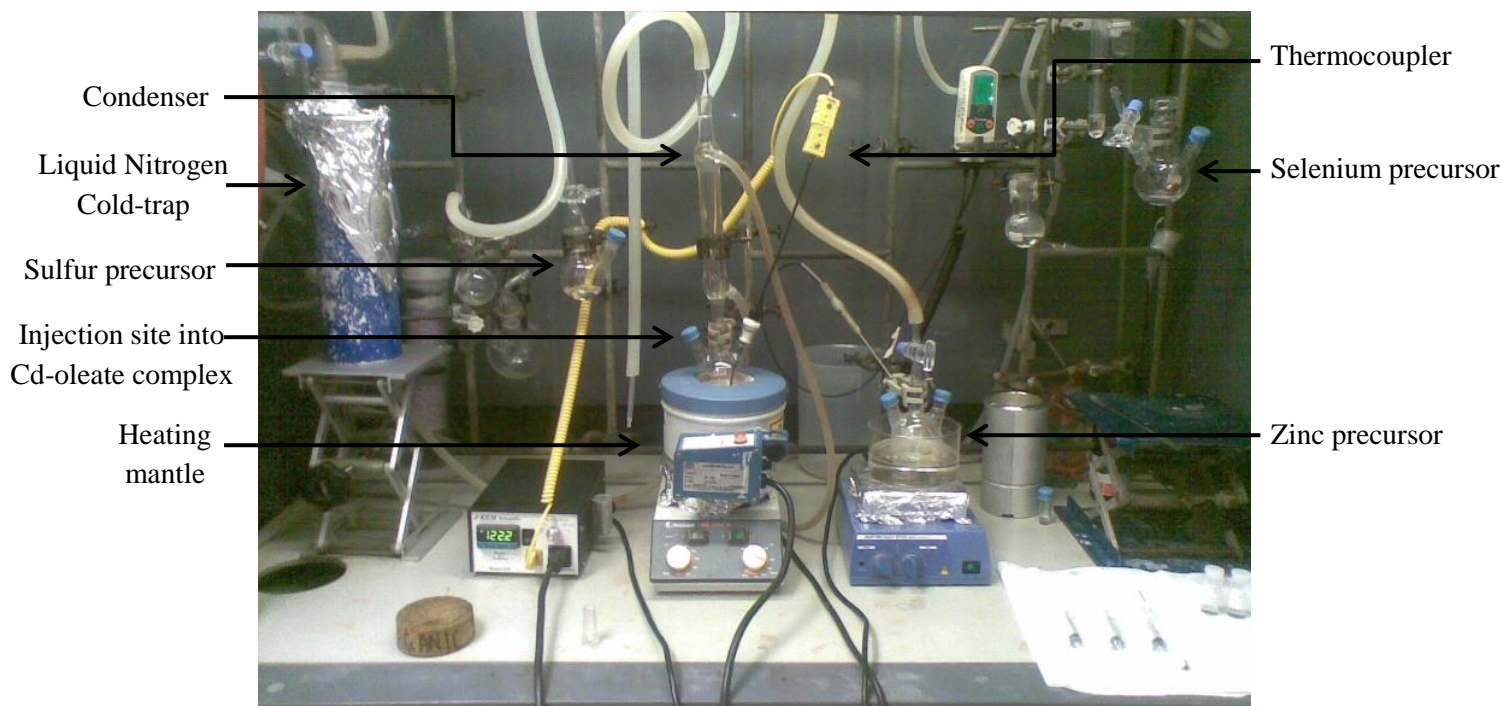


Figure 2.1. General setup for the organometallic synthesis of CdSe/ZnS core-shell QDs.

The temperature of the Zn-TOP mixture was then lowered to 90 °C. At the same time, the CdSe solution was reheated to 90 °C. At this point, the TOP-Zn was added and allowed to mix for 10 min. Thereafter, the TOP-S was added to the reaction mixture and this was followed by growth of the ZnS nanoparticle shell for one hour. Aliquots (0.1 ml) were extracted at 30 min and 60 min and dissolved in hexane. The reaction was then stopped and allowed to cool down to room temperature. The CdSe/ZnS quantum dot sample was stored at 4 °C.

2.4.2. Precipitation of the CdSe/ZnS core-shell QDs

The quantum dot sample generated in **Section 2.4.1** was dissolved in a small amount of hexane (1 ml). This solution was then transferred to clean 2 ml eppendorf tubes, vortexed and centrifuged at 14 500 x g for 10 min. The supernatant from all the eppendorf tubes were transferred to a clean glass beaker and the pellets were discarded. Acetone was added to the

supernatant until a cloudy solution was achieved. This solution was then transferred to clean 2 ml eppendorf tubes, vortexed and centrifuged at $14\,500 \times g$ for 10 min. The clear supernatant was discarded and a few drops of hexane were added to the pellet in one of the eppendorf tubes. This suspension was vortexed and transferred to the next eppendorf. The pellets were all collected in this manner until one suspension remained. A few drops of acetone were added to the suspension, at this point, the solution became cloudy. The solution was vortexed and centrifuged at $14\,500 \times g$ for 10 min. The supernatant was discarded and the pellet was weighed and stored at $4\text{ }^{\circ}\text{C}$, in the dark, until further use.

2.4.3. Characterisation of CdSe/ZnS core-shell QDs

2.4.3.1. PL spectroscopy

The PL spectra were obtained using the HORIBA Nanolog FL3-22-TRIAX spectrometer that used a CCD detection system. Dilute solutions of the CdSe/ZnS core-shell QDs in hexane were placed in 1 cm quartz cuvettes and their corresponding fluorescence were measured. This is a non-destructive technique that can provide information about semiconducting material. Upon exposure of the nanomaterial to light, the PL (emitted light) gets stimulated by a higher energy than that of the luminescent light and an emission spectrum is formed and analysed computationally (Seyhan, 2003).

2.4.3.2. High resolution transmission electron microscopy

High resolution TEM micrographs were obtained on a field emission TEC NAI F20 TEM microscope. One drop of a dilute solution of CdSe/ZnS core-shell QDs in hexane was placed onto a copper grid, supported by a thin film of amorphous carbon. This technique uses electrons that are shot through the sample at a high acceleration voltage. Changes in the electron beam due to scattering discharged by the sample are then measured. This interaction

between the electrons and the sample, at that point, produces an image. The difference in contrast between the sample and the background Cu grid, provides direct information about the nanoparticle morphology (Qi *et al.*, 2001 & Rao and Biswas, 2009).

2.4.3.3. Energy dispersive x-ray spectroscopy

The EDS spectrum was obtained using a field emission TEC NAI F20 TEM microscope. The same samples from **Section 2.4.3.2** were used. EDS is a characterisation technique that provides an elemental and chemical analysis of the nanomaterial being probed (Rao and Biswas, 2009). EDS relies on the unique atomic structure ascribed to every element, in such a way that the x-ray spectrum emitted for the different atomic structures, are clearly discernible from one element to another. The spectrum is formed by excitation of electrons in the inner shell (lower energies). The excited electrons move to a higher energy state, subsequently creating vacant shells in the electronic structure of the atoms being probed. Electrons from the outer shells (higher energies) replenish the vacant shells; and the difference in energy between the higher and lower energy shells are emitted as x-rays. The x-rays are then measured by an energy dispersive spectrometer (Russ 1984 & Rao and Biswas, 2009).

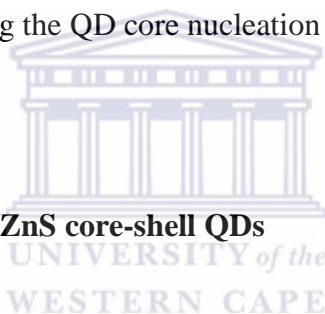
2.4.4. Ligand exchange

The quantum dot pellet generated in **Section 2.4.2** was dissolved in a 1.65 mM solution of L-cysteine (pH 8) and sonicated at 50 W and 60 Hz for 1 min, then placed on ice for 30 sec. This was repeated until a 15 min sonication cycle was completed. The water-soluble L-cysteined capped QDs were stored at 4 °C, in the dark, until further use.

2.5. Results and discussion

2.5.1. Synthesis of CdSe/ZnS core-shell QDs

Highly luminescent and monodispersed CdSe/ZnS core-shell QDs were synthesised using an organometallic approach, as described in **Section 2.4.1** (Boatman and Lisensky, 2005). CdO, Se, Zn undecylated and sulfur powder were used as the source for the Cd, Se, Zn and S precursors, respectively. 1-Octadecene (ODE) served as a solvent for the Cd-oleate mixture and the ODE/TOP mixture served as a solvent for the remaining precursors. Oleic acid (OA) provided a protective capping layer. It was also selected for its dual function, that is, primarily a stabilising ligand for Cd to form a highly reactive Cd-oleate complex. Secondly, OA served as an accelerator during the QD core nucleation process (Zou *et al.*, 2010).



2.5.2. Characterisation of CdSe/ZnS core-shell QDs

2.5.2.1. Introduction

The unique properties exhibited by nanoparticles and QDs in particular, are attributed to their physicochemical properties. Therefore, determining these characteristics plays an important role in understanding their behaviour and subsequent application in biological systems (Zhang and Clapp, 2011). Since much attention has been drawn to QDs as a result of their unique optical properties; from the literature, the most frequently reported characterisation techniques employed include (1): UV-Vis spectroscopy to measure absorbance which induces the electronic transition from the ground to the excited state and (2): PL spectroscopy to measure fluorescence which is when the electronic transition occurs from the excited to the ground state. Additionally, transmission electron microscopy (TEM) provides detailed morphological information by interrogation of electron diffraction patterns. TEM also serves

as a good validation approach for other methods. EDS is another technique employed for elemental analysis (Dabbousi *et al.*, 1997 & Boatman and Lisensky, 2005 & Pechstedt *et al.*, 2010).

2.5.2.2. PL properties of CdSe/ZnS core-shell QDs

Medintz *et al.*, (2005) and Pong *et al.*, (2008) reported QDs synthesised from CdSe cores coated with a ZnS shell, as the best suited QDs for biological applications because the chemistry of these QDs are extensively researched and understood. As previously mentioned, the ZnS layer serves to (1) passivate the core surface, (2) safeguard it from oxidation, (3) inhibit Cd/Se leaching into the buffer solution and (3) improving PL yield. PL spectroscopy aids in providing valuable information about the as-synthesised QDs optical properties; which in turn helps to interpret whether or not the aforementioned properties were achieved (Medintz *et al.*, 2005 and Pong *et al.*, 2008).

The objective of the synthesis was to obtain green emitting fluorescent nanoparticles. The optimised time for the experiments was 8 min which demonstrated sufficient fabrication of CdSe cores with wavelength emissions at ~510 nm. This finding agrees with Huy *et al.*, who demonstrated that extended QD core growth times induce a decrease in PL intensity (Huy *et al.*, 2011). This occurs as a result of particles that are highly susceptible to re-dissolution or bleaching prompted by the heat. **Figure 2.2** shows the PL spectrum used (1): to investigate whether the ZnS was successfully coated onto the CdSe QDs, (2): to define the size distribution; and (3): to determine the wavelength emissions of the nanoparticles synthesised in **Section 2.4.1**.

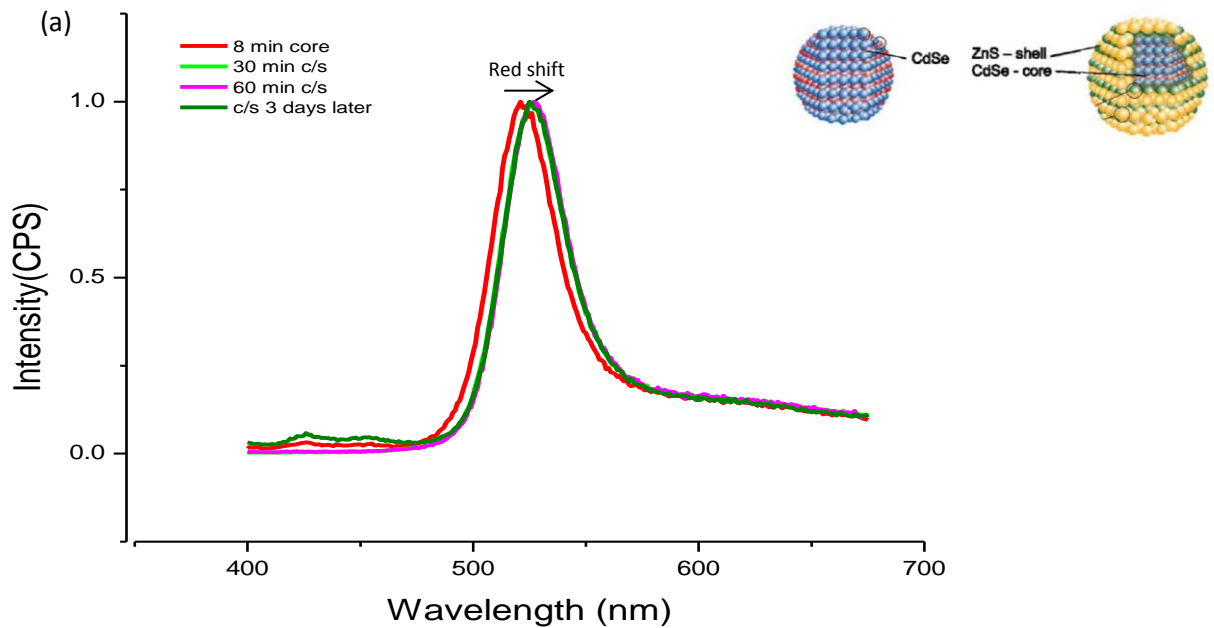
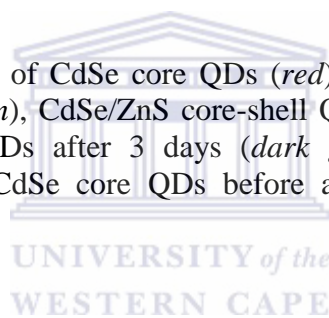


Figure 2.2. PL spectra of CdSe core QDs (*red*), CdSe/ZnS core-shell QDs after 30 min (*light green*), CdSe/ZnS core-shell QDs after 60 min (*pink*) and CdSe/ZnS core-shell QDs after 3 days (*dark green*). The inset shows a schematic diagram of CdSe core QDs before and after coating with ZnS (Angell, 2011).



No significant differences were observed between the 30 min and 60 min ZnS coating time points. However, a red shift in the emission wavelength from the core to core-shell structure (*green and pink peaks*) was observed. This suggests that an increase in particle size occurred, and therefore, successful ZnS coating of CdSe QDs was achieved as similarly reported (Dabbousi *et al.*, 1997 & Pechstedt *et al.*, 2010).

The narrow and sharp PL peaks depicted that both the CdSe core and CdSe/ZnS core-shell QDs had a narrow size distribution. Additionally, literature suggests that the surface passivation of the CdSe core with a ZnS coating should result in a higher quantum yield by approximately 50 % (Dabbousi *et al.*, 1997). QDs with smaller diameters usually have very large surface-to-volume ratios and the presence of surfactants such as TOP are subjected to broad deep trap emissions as a result of incomplete surface passivation (Dabbousi *et al.*, 1997

& Jones *et al.*, 2003). The ZnS coating should therefore function as a suppressor of these trap emissions by passivation of the surface trap sites within the crystalline structure (Dabbousi *et al.*, 1997). This in turn produces a PL subjected to band-edge recombination and thus, higher quantum yield (Jones *et al.*, 2003).

It is important to note the wavelengths at which these particles emit light. Green fluorescent molecules have emission profiles near 500 nm (Bruchez *et al.*, 1998). The CdSe/ZnS core/shell QDs emitted light with a wavelength of ~525 nm, as described in **Section 2.4.1**.

2.5.2.3. Transmission electron microscopy

To directly investigate the size distribution and morphology of QDs, TEM or HR-TEM may be employed. For biological applications, the importance of producing QDs with particular structural properties would facilitate the ease of functionalising the nanoparticles with biomolecule counterparts (Zhang and Clapp, 2011).

The HR-TEM micrograph for the CdSe/ZnS core-shell QDs is shown in **Figure 2.3**. The micrograph shows that the QDs are relatively monodispersed and spherical in shape. The **inset of Figure 2.3** demonstrates that poor lattice fringes were resolved, revealing that the structural quality of the QDs were not of high quality. This may be as a result of high lattice mismatches between the core and shell materials during the growth phase (Qi, 2001 & Zeng *et al.*, 2009).

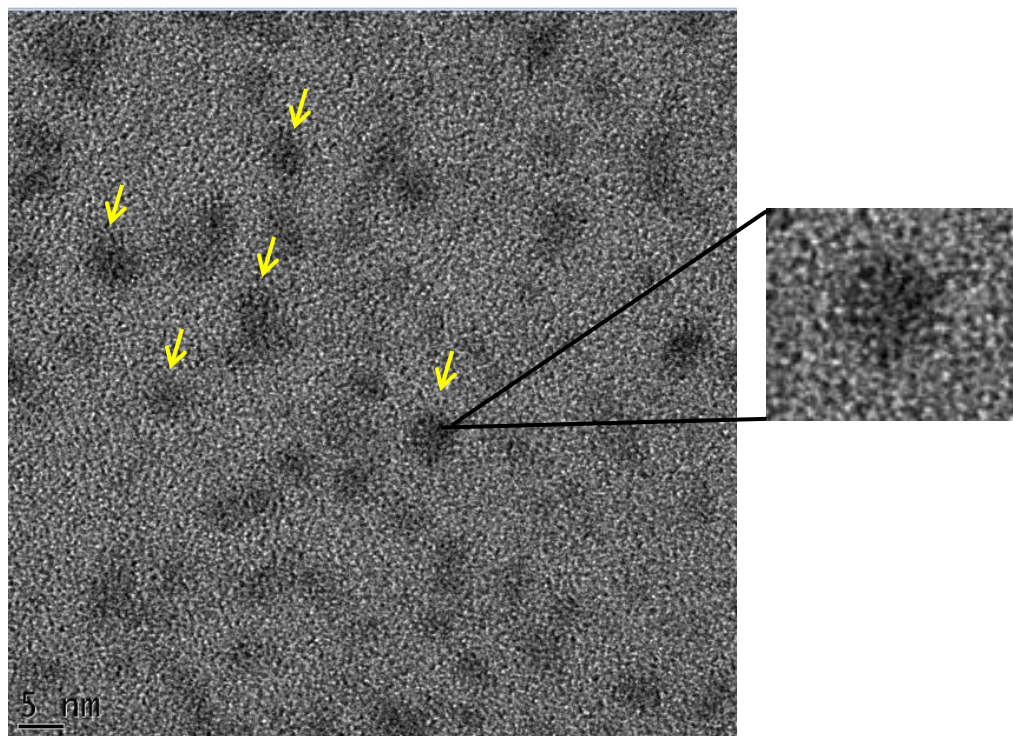


Figure 2.3. High Resolution-TEM micrograph of CdSe/ZnS core-shell QDs.

2.5.2.4. EDS

Physical characterisation of nanomaterials may be achieved at different levels. To confirm the composition of the QDs prepared, the EDS analysis was carried out. The EDS spectrum showed the presence of all the four elements, Cd, Se, Zn and S (**Figure 2.4**).

After successful characterisation by PL spectroscopy, HR-TEM and EDS, it was demonstrated that nearly monodispersed and green fluorescent CdSe/ZnS core-shell QDs were synthesised using an organometallic approach. The results obtained were satisfactory proven to proceed with ligand exchange to solubilise the QDs for a biological environment.

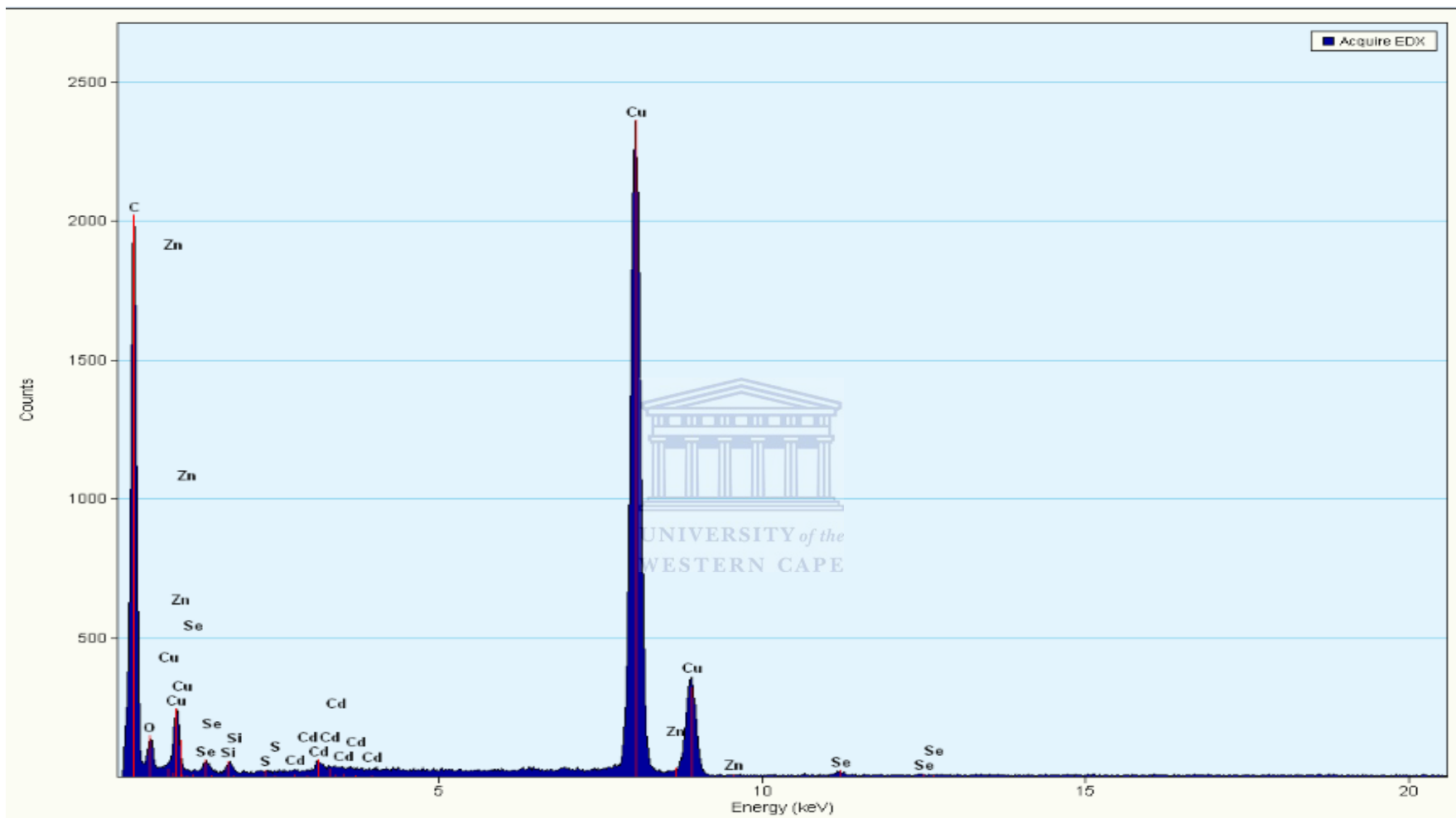
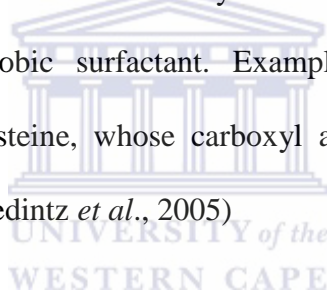


Figure 2.4. EDS spectrum of the as prepared CdSe/ZnS core-shell QDs.

2.6. Water soluble CdSe/ZnS core-shell QDs

2.6.1. Introduction

The organometallic approach produces QDs stabilised by hydrophobic surfactants and therefore an important step is then to ensure that these QDs are rendered water-soluble. This may be achieved by surface modification with hydrophilic or amphiphilic moieties that would facilitate its application in a biological environment (Zhang and Clapp, 2011). The high-temperature synthesis lack intrinsic aqueous solubility, subsequently; phase-transfer to an aqueous solution is required through one of two strategies, that is, encapsulation or ligand exchange. Encapsulation relies on hydrophobic adsorption onto the TOP capped QDs, whereas; ligand exchange relies on mass action by means of heterobifunctional ligands that serve to displace the hydrophobic surfactant. Examples of such ligands include 3-mercaptopropionic acid or L-cysteine, whose carboxyl and amine moieties, respectively, renders the QD water-soluble (Medintz *et al.*, 2005)



2.6.2. Ligand Exchange

Ligand exchange approaches reported for L-cysteine capped CdSe/ZnS QDs (Cys-QD) generally involved transferring the QDs from the organic phase to the aqueous phase as described above, however, the resultant Cys-QDs were only stable for 24 hours. Precipitated Cys-QDs were observed as macroscopic aggregates formed as a result of cysteine oxidation, consequently forming cysteine dimers (cystine) that are incapable of binding to the QD surface (Liu *et al.*, 2007). An alternative capping strategy proposed by Carrillo-Carrion *et al.*, produced bio-compatible and more stably dispersed Cys-QDs which showed a decline in

fluorescence intensity after 2 days, though the dispersion was stable for at least a month (Carrillo-Carrion *et al.*, 2009).

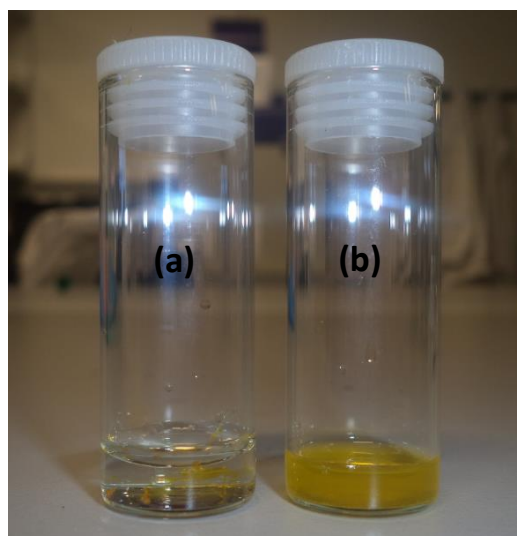


Figure 2.5. Ligand exchange using L-Cysteine (a) CdSe/ZnS core-shell QDs before sonication and (b) after sonication

Figure 2.5 shows the development of water-soluble Cys-QDs using the method described by Carrillo-Carrion *et al.*, described in **Section 2.4.3**. Prior to sonication, the TOP capped CdSe/ZnS core-shell QDs remained in its pelleted form, clearly demonstrating the hydrophobicity. However, after sonication (ligand exchange), the Cys-QDs appear well dispersed in the aqueous solution, indicative of a successful ligand exchange. The water-soluble QDs produced in this section were of satisfactory quality to proceed with biological application, when characteristically compared to those discussed above by Carrillo-Carrion *et al.*, 2009.

Chapter Three: Selective eradication of cancer cells using peptide directed QDs to deliver a pro-apoptotic peptide

3.1. Introduction

The efficiency of any cancer treatment is directly related to and measured by its capacity to reduce or eradicate tumours and minimally, if at all damage healthy tissue (Byrne *et al.*, 2008). Considering this, the therapeutic goal of cancer is to selectively target and kill cancerous cells (Haglund *et al.*, 2009 & Sioud and Mobergslien, 2012 & Thundimadathil, 2012). Conventional chemotherapeutic drugs lack the aforementioned ability as a result of non-specific distribution of the drug. Consequently, giving rise to dose-related systematic toxicities, thereby, restricting the amount of drug to be administered and in turn leading to inadequate therapeutic effects (Allen and Cullis, 2004 & Wang *et al.*, 2009). For this reason, an alternative strategy is required. Nanoparticle delivery systems offer an improved alternative due to their ability to interact at the cellular level with a great degree of specificity (Byrne *et al.*, 2008 & Singh and Lilard, 2009).

3.2. Objective of this chapter

The objective of this chapter was to, respectively, bi-conjugate the commercially available amino Qdot525 (Qdot525) and the previously synthesised Cys-QDs (Chapter 2) to the LTVSPWY (p.L) and Smac peptides. Then carry out a comparative study to relate the efficiency of the Cys-QDs to the Qdot525 by evaluating whether the respective QD peptide bi-conjugates (Qdot525/p.L+Smac or Cys-QD/p.L+Smac) selectively target and eradicate cancer cells.

3.3. Materials and suppliers

2X Trypsin	Life Technologies
Amino Qdot®525 ITK™	Life Technologies
BM cyclin	Roche
Boric acid	Sigma-Aldrich
Dimethyl sulfoxide (DMSO)	Sigma-Aldrich
Dulbecco's Modified Eagles Media (DMEM)	Whitehead Scientific
1-ethyl-3-(3-dimethylaminopropyl) carbodiimide (EDC)	Sigma-Aldrich
Ethanol	Merck
Fetal Bovine Serum (FBS)	Biochrome
Fluoroshield with DAPI	Sigma-Aldrich
LTVSPWY peptide	Anaspec
N-acetyl-D-erythro-sphingosine (C2 Ceramide)	Sigma-Aldrich
Nucblue Live Cell Stain	Life Technologies
Paraformaldehyde	Sigma-Aldrich
Penicillin/streptomycin	Whitehead Scientific
PD-10 purification column	GE Healthcare
Phosphate buffered saline (PBS)	Whitehead Scientific
Smac/DIABLO peptide	Anaspec
Sodium Hydroxide	Merck
Triton X-100	Sigma-Aldrich



3.4. Solutions and buffers

3% Bovine Serum Albumin (BSA): 0.3 g/ml BSA was prepared in PBS.

3.5. Methods

3.5.1. Cell culture

HT29 and HeLa cells were cultured in Dulbecco's Modified Eagles Medium (DMEM), supplemented with 10 % penicillin/streptomycin (Life Technologies) and 10 % Fetal Bovine Serum (FBS) (Biochrome).

3.5.2. Thawing of cells

Vials containing the frozen cells were removed from the -150 °C freezer and allowed to thaw at room temperature. Cells were then transferred to a 15 ml tube containing 3 ml DMEM and the latter transferred into a 25 cm² tissue culture flask. The flask was placed in a water jacketed CO₂ incubator (Labotec) at 37 °C and 5 % CO₂ until 60-90 % confluency was reached.

3.5.3. Trypsinization of cells

Once the cells reached the desired confluency, trypsinization was carried out as follows:

The DMEM in the flask was decanted. Thereafter, the cells were washed with 1 X Phosphate buffered saline (PBS). The PBS was then discarded and the cells were trypsinized with the addition of 1 X trypsin and incubated in a water jacketed CO₂ incubator at 37 °C for 2-3 min. DMEM was added to the cells to inactivate the trypsin. Cells were collected by centrifugation at 3000 x g.

3.5.4. Freezing of cells

Once the cells reached the desired confluency, the cells were removed by trypsinization as described above in **Section 3.5.3**. The cell pellet generated from trypsinization was prepared for long-term storage. The cell pellet was resuspended in DMEM containing 10 % DMSO, and aliquoted into 2 ml cryo-vials and stored at -150 °C.

3.6. Dose response curves

3.6.1. Seeding of cells

HT29 cells were cultured and trypsinized as described in **Section 3.5.1 and 3.5.3**. The cells were counted using the Countess Automated Cell Counter (Invitrogen). The cells were seeded in to 96-well cell culture plates at a cell density of 1×10^5 cells/ml. The 96-well cell culture plates were placed into a water jacketed CO₂ incubator at 37 °C for 24 hrs.

3.6.2. QD Treatment

After 24hrs of culturing, the cells were treated with varying concentrations of QDdot525 (Invitrogen) or Cys-QD (Chapter 2) for 24 hrs in a water jacketed CO₂ incubator at 37 °C. The treatments were performed in triplicate. After the 24 hrs treatment, the WST-1 Cell Proliferation Reagent (10 µl/well) was added to the respective wells. The cells were further incubated in a water jacketed CO₂ incubator at 37 °C. The 96-well cell culture plates were agitated for 1 min and absorbance readings were obtained at 440 nm and 620 nm using a Spectrophotometer (BMG labotec).

3.7. Bi-conjugation of QDs to peptides

The reagents as listed in **Tables 3.1 and 3.2**, were added to a clean amber (light protective) glass vial. The reaction mixture was vortexed for 2 hrs at room temperature. Two other

conjugations were setup in a similar manner, in the absence of the Smac peptide and used as controls. The QD peptide bi-conjugates generated from this reaction were: (1) Qdot525/p.L+Smac, (2) Qdot525/p.L, (3) Cys-QD/p.L+Smac and (4) Cys-QD/p.L.

Table 3.1. Bi-conjugation of the Qdot525 to the p.L and Smac peptides

Qdot525/p.L+Smac	Qdot525/p.L	Stock concentration	Final concentration
Borate Buffer (pH 8.5)	Borate Buffer (pH 8.5)	50mM	50 mM
Amino-Qdot525	Amino-Qdot525	8 μ M	0.25 μ M
p.L peptide	p.L peptide	11595 μ M	50 μ M
Smac peptide	-	10602 μ M	50 μ M
EDC	EDC	50 μ M	0.375 μ M

Table 3.2. Bi-conjugation of the Cys-QD to the p.L and Smac peptides

Cys-QD/p.L+Smac	Cys-QD/p.L	Stock concentration	Final concentration
Borate Buffer (pH 8.5)	Borate Buffer (pH 8.5)	50mM	50 mM
Cys-QD	Cys-QD	14400 μ g/ml	350 μ g/ml
p.L peptide	p.L peptide	11595 μ M	50 μ M
Smac peptide	-	10602 μ M	50 μ M
EDC	EDC	50 μ M	0.375 μ M

3.8. Desalting of the QD peptide bi-conjugates by gel filtration

The bi-conjugates were subjected to purification using the PD10 desalting column (GE Healthcare) according to the manufacturer's instructions:

The cap at the bottom of the column was removed and the column storage solution was poured off. The sealed end of the column was cut off. The column was then equilibrated by addition of the equilibration buffer (Borate buffer, pH 8.5). The buffer was allowed to migrate into the column bed and the flow through was discarded. This was repeated four

times. The QD-peptide bi-conjugates were added to the respective columns. The QD-peptide bi-conjugates were allowed to migrate into the column bed. The volume was adjusted to 2.5 ml, by addition of the equilibration buffer. The buffer was then allowed to migrate into the column bed. The flow through was discarded. Clean glass vials were placed under the columns for sample collection. The bi-conjugates were collected by addition of the elution buffer (1 X PBS, pH 7.4) at 1000 µl elutes. Aliquots of 100 µl were placed into PCR tubes. An aliquot (100 µl) of the unconjugated QD samples (Qdot525 and Cys-QDs) were included as controls. Images were captured under UV-light (UVP) and the desalted bi-conjugates were stored at 4 °C until further use.

3.9. Immunocytochemistry

3.9.1. Seeding of cells

HT29 and HeLa cells were cultured and trypsinized as described in **Section 3.5.1 and 3.5.3**. The cells were counted using the Countess Automated Cell Counter (Invitrogen). The cells were seeded onto sterilised coverslips in 6-well cell culture plates at a cell density of 2×10^5 cells/ml. The 6-well cell culture plate was placed in a water jacketed CO₂ incubator at 37 °C and the cells cultured until 50 – 60 % confluency.

3.9.2. Fixation and permeabilisation

Once the cells reached the desired confluency, the media was removed from the cells in 6-well cell culture plates using a pipette. The cells were washed twice with 1 X PBS. The PBS was then discarded and 4 % formaldehyde was added to each well and left for 20 min at room temperature to allow cells to fix to the coverslips. The PBS was then discarded and 0.1 % Triton X-100 was added to each well and left for 5 min to allow permeabilisation of the cell membrane. This was followed by washing the cells twice with 1 X PBS.

3.9.3. Fixed cell staining

The washed cells were then incubated with the respective QD peptide bi-conjugates: Qdot525/p.L+Smac, (2) Qdot525/p.L, (3) Cys-QD/p.L+Smac and (4) Cys-QD/p.L for 1 hr at room temperature. A drop of Fluoroshield DAPI mounting media (Sigma-Aldrich) was placed onto labelled microscope slides. The cells were washed 3 times with PBS and dried by blotting the edges of the coverslip on paper towel. The coverslips were transferred onto the mounting media with the cell-side faced down. The images were captured at 100 X magnification under oil immersion using the fluorescent Carl Zeiss LSM 780 Confocal microscope with Elyra S.1 super resolution platform (Carl Zeiss).

3.9.4. Live cell staining

Cells were seeded as described in **Section 3.9.1**. Once the cells reached the desired confluency, the media was removed from cells in 6-well cells culture plates using a serological pipette. The cells were washed twice with 1 X PBS. The PBS was then discarded and the cells were incubated with the respective QD peptide bi-conjugate for 24 hrs in a water jacketed CO₂ incubator at 37 °C. The staining medium was then removed using serological pipette and the cells were washed four times with 1 X PBS. The cells were then fixed as described in **Section 3.9.2**. A drop of Nuclblue Live Cell Stain was placed onto labelled microscope slides and the cells were mounted and visualised as described in **Section 3.9.3**.

3.10. Cytotoxicity assay

HT29 and HeLa cells were seeded as described in **Section 3.9.1**. After 24 hrs of culturing, the cells were treated with the respective QD peptide bi-conjugates (**Section 3.7**) in the presence or absence of ceramide (60 µM) for 24 hrs in a water jacketed CO₂ incubator at 37 °C. The treatments were performed in triplicate. After the 24 hr treatment, WST-1 Cell Proliferation

Reagent (10 μ l/well) was added to the respective wells. The cells were further incubated for 2 hrs in a water jacketed CO₂ incubator at 37 °C. The 96-well cell culture plates were agitated for 1 min and analysed using a spectrophotometer (BMG labotec).



3.11. Results and Discussion

3.11.1. Dose response curves to determine optimal QD concentration

To determine a good response model for the drug delivery system, a non-hazardous dosage of the QDs must be obtained. Therefore using a dose response curve, the lethal concentration at ~50 % (LD_{50}) of the QDs and the appropriate, non-hazardous concentration of the QDs required for application in the QD peptide bi-conjugate can be extrapolated. Since the aim of the targeted drug delivery system developed in this study is to sensitise the cells to treatment with ceramide, it is important to ensure that the QDs do not induce toxicity. To accomplish this, HT29 cells were seeded and treated as described in **Sections 3.6.1 and 3.6.2**. **Figure 3.1** shows the dose response curves for HT29 cells after the 24 hr treatment.

Cellular viability was assessed using the WST-1 Cell Proliferation (Roche) colometric assay. **Figure 3.1** illustrates that a decrease in cell viability is directly proportional to an increase in QD concentration for both the Qdot525 and the Cys-QDs. The LD_{50} values obtained were ~0.8 μM and ~720 $\mu\text{g/ml}$ for Qdot525 and Cys-QDs, respectively. Based on this dose response curve, it was decided to use a concentration below the LD_{50} , 0.25 μM and 350 $\mu\text{g/ml}$ for the Qdot525 and Cys-QDs, respectively.

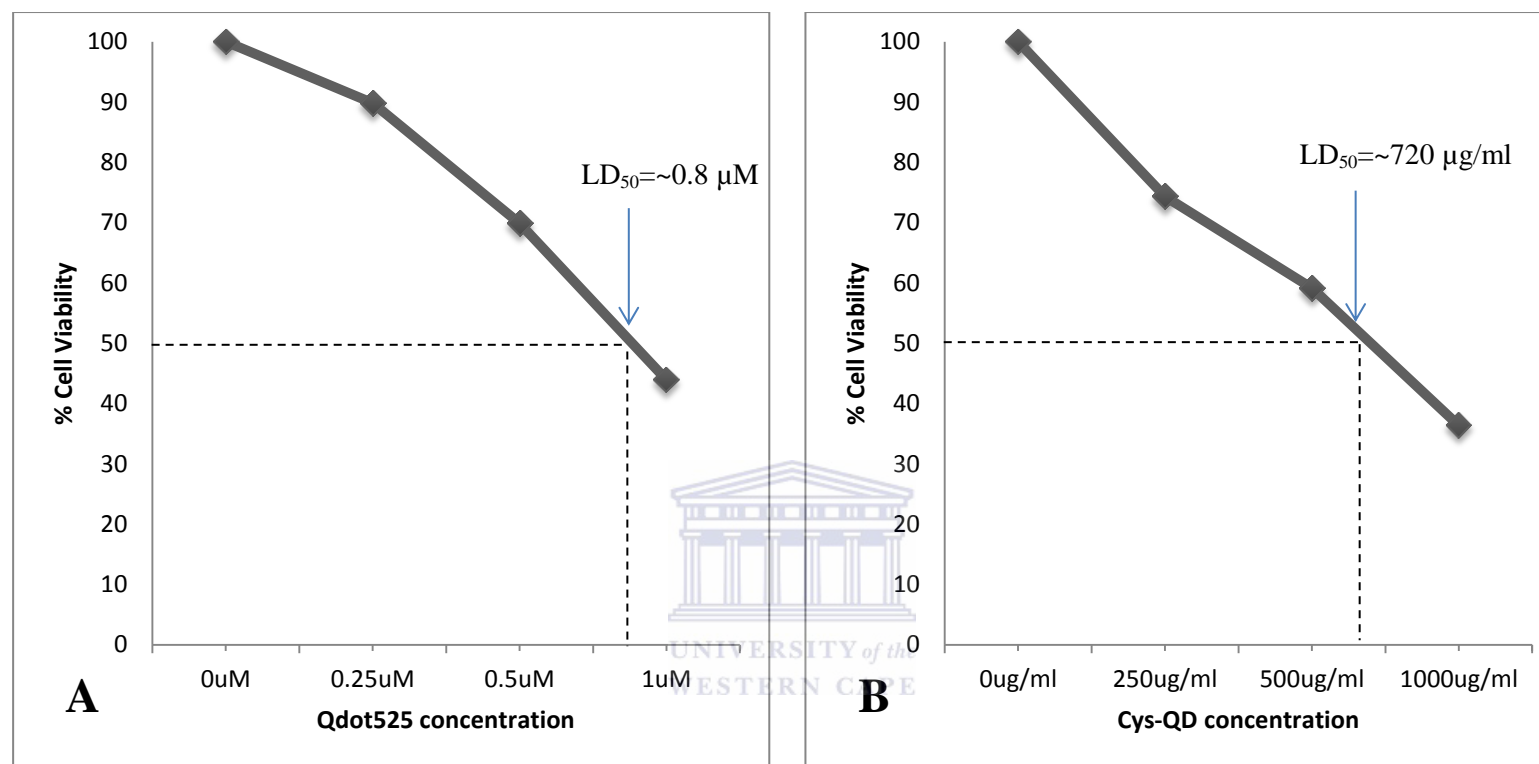


Figure 3.1. Dose response curve of the Qdot525 (A) and Cys-QDs (B). HT29 cells were subjected to treatment with the Qdot525 or the Cys-QD for 24 hrs. Subsequently, the cell viability was determined using the WST-1 Cell Proliferation colometric assay. The data was obtained in triplicate and used to construct dose response curves for the respective QDs (mean ± SD; n=3).

3.11.2. Bi-conjugation of QDs to peptides using EDC chemistry

The specificity of a nanoparticle-based drug delivery system can be achieved by cancer specific peptides; owing to its high-affinity sequences that are easy to conjugate to its' counterparts. Furthermore, its' small size that permits a good degree of tissue penetrability and drug carrying capacity, negligible immunogenicity; and a considerable level of in vivo stability (Jaracz *et al.*, 2005 & Li and Cho, 2012). In order to facilitate the use of a drug delivery system, the respective moieties are required to be chemically linked (Hermanson, 2013). EDC is cross-linker most often employed to mediate the bi-conjugation of amino and carboxylate groups (Zhang and Clapp, 2011 & Vashist, 2012).

The objective of this section was to generate four bi-conjugates, namely, (1) Qdot525/p.L+Smac, (2) Qdot525/p.L, (3) Cys-QD/p.L+Smac and (4) Cys-QD/p.L. This was achieved using EDC chemistry as described in **Section 3.6** and schematically illustrated in

Figure 3.2.

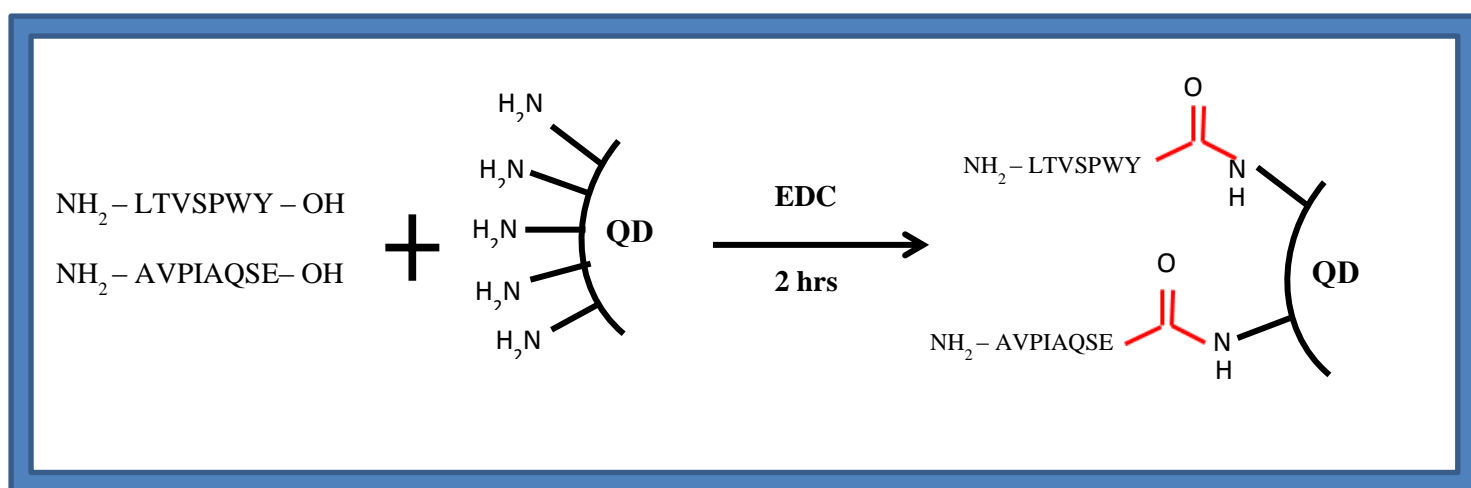


Figure 3.2. Schematic diagram illustrating cross-linking of amine functionalised QDs with p.L and Smac. EDC activates the carboxylate groups present on the peptides and in the presence of the amine functionalised QDs, a covalent bond is formed.

3.11.3. Desalting of the bi-conjugates using gel filtration

The bi-conjugates prepared in **Section 3.7** were then subjected to desalting using the PD10 gel filtration column (GE Healthcare) as described in **Section 3.8**. The objective of this section was to determine which fraction contained the QD peptide bi-conjugate. This was determined by comparing the fluorescence intensities of the various elutes, as demonstrated in **Figure 3.3**.

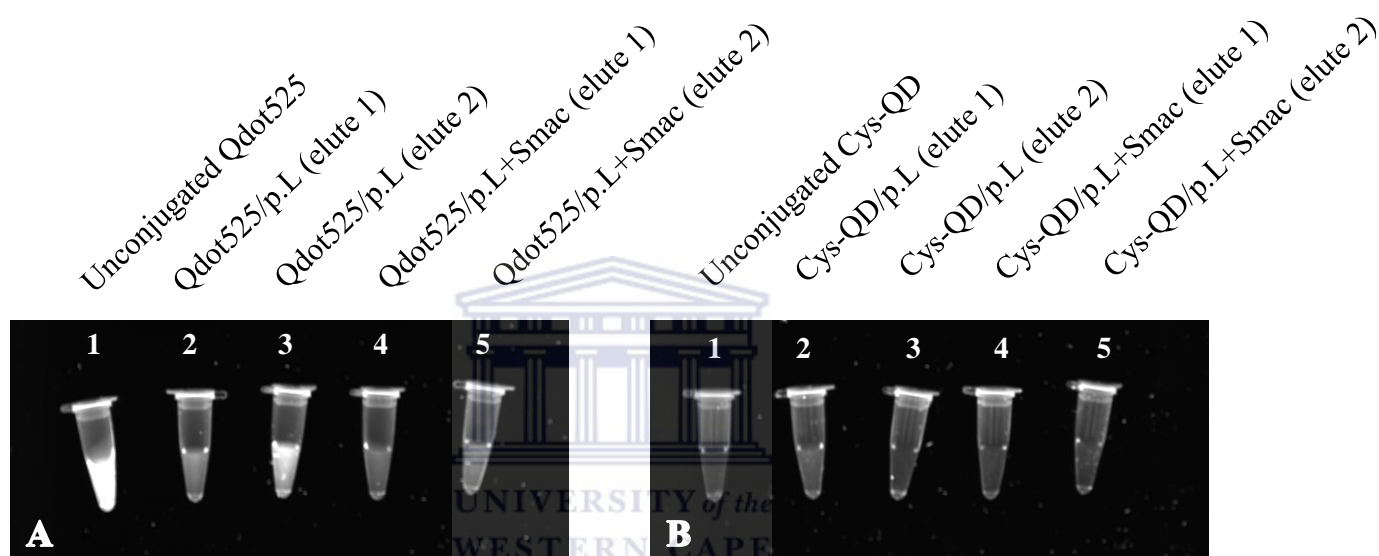


Figure 3.3. Desalted QD peptide bi-conjugates. In (A) Qdot525 peptide bi-conjugates and (B) Cys-QD peptide bi-conjugates, Lane 1 represent the unconjugated QDs. Lanes 2 and 3 represent elutes 1 and 2, respectively for the QD/p.L bi-conjugates. Lanes 4 and 5 represent elutes 1 and 2, respectively for the QD/p.L+Smac bi-conjugates. Images were captured using the UVP system.

The unconjugated Qdot525 sample showed the highest fluorescence. This was expected, since these QDs were in a more concentrated form. The Qdot525/p.L and Qdot525/p.L+Smac elute 2 had a higher fluorescence intensity than that of their elute 1 counterparts. This suggests that elute 2 contained most of the Qdot525 peptide bi-conjugates. The unconjugated Cys-QDs fluorescent signal was not as bright as that of the unconjugated Qdot525 sample. Contrary to the Qdot525 peptide bi-conjugates, the Cys-QD/p.L elute 1 had a higher

fluorescent signal than that of Cys-QD/p.L elute 2, suggesting that more of the Cys-QD peptide bi-conjugates were present in this fraction. Overall, the Cys-QD had a very poor fluorescent signal which may be accounted for by low concentrations (350 µg/ml) used in the bi-conjugation reactions. Nonetheless, the presence of a fluorescent signal in multiple fractions, confirmed the presence of the QDs, therefore, suggesting the presence of the QD peptide bi-conjugates. Based on the fluorescence intensities of the various fractions observed in **Figure 3.3**, elute 2 for the Qdot525 peptide bi-conjugates and elute 1 for the Cys-QD peptide bi-conjugates were used for further experiments.

3.11.4. Evaluating the cytotoxicity of the QD bi-conjugate targeted delivery system using the WST-1 Cell Proliferation assay

The objective of this section was to evaluate the cytotoxicity of (1) Qdot525/p.L+Smac and (2) Cys-QD/p.L+Smac by combinatorial treatment with ceramide. This was achieved by seeding and treating the cells as described in **Section 3.9.1 and 3.9.2**.

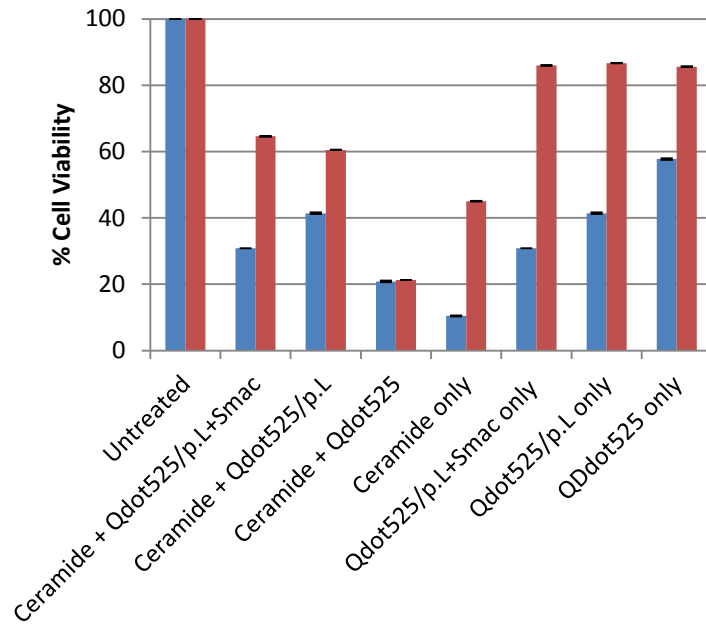
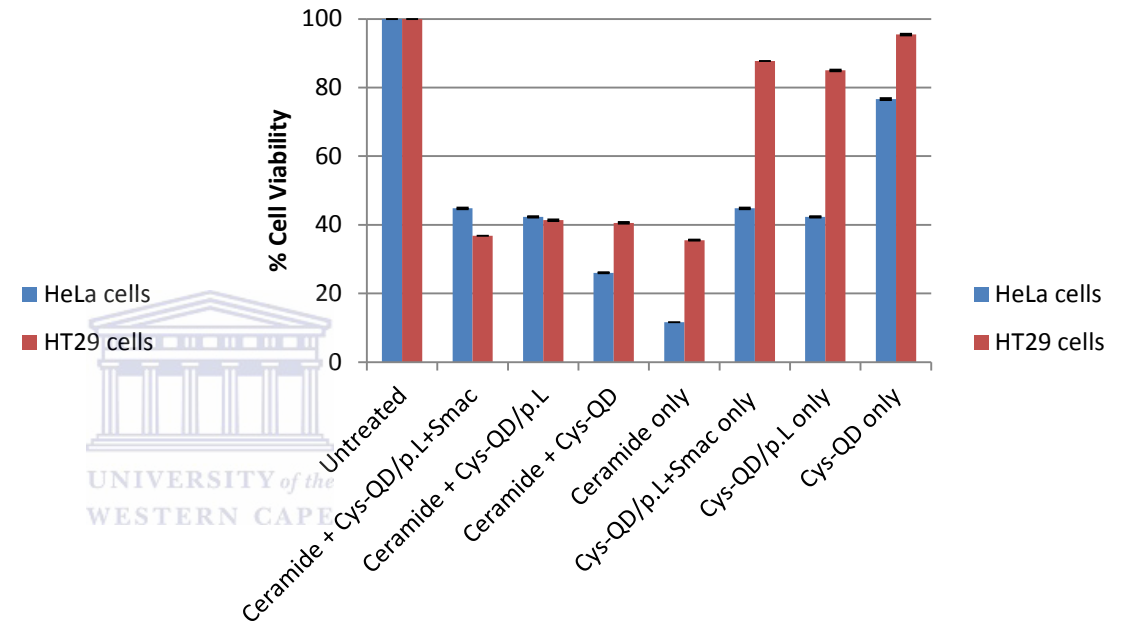
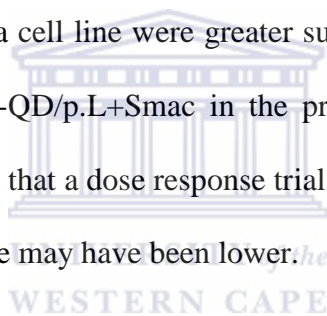
A**B**

Figure 3.4. Evaluating the cytotoxicity of the targeted drug delivery system. HT29 and HeLa cells were subjected to treatment with the Qdot525 peptide bi-conjugate or the Cys-QD peptide bi-conjugate in the presence or absence of ceramide for 24 hrs. Subsequently, the cell viability was analysed using the WST-1 colometric assay. The data was obtained in triplicate and used to construct dose response curves for the respective QDs (mean \pm SD; n=3). Error bars represent calculated standard error of the means.

Figure 3.4 shows the cytotoxic profile of the respective QD/p.L+Smac bi-conjugates. The Qdot525/p.L+Smac bi-conjugate did not enhance the apoptotic effect of ceramide. On the contrary, a degree of cytoprotection or anti-apoptotic effect was observed for HT29 cells as illustrated by the 20 % increase in cell viability conferred by the Qdot525/p.L+Smac bi-conjugate (65 % cell viability) as compared to the ceramide only control (45 % cell viability). It is possible that the Qdot525 peptide bi-conjugates interacted with ceramide and induced an inhibitory effect on ceramide induced apoptotic signalling because the Qdot525/p.L+Smac bi-conjugate failed to induce statistically significant cell death when treated without ceramide (86 % cell viability). The cytoprotective effect observed may also be due to insufficient concentrations of the Smac peptide. This may be as a result of a poorly controlled conjugation setup in that, there may have been competitive conjugation between the p.L and Smac peptides for the amine groups present on the QD surface, potentially resulting in insufficient quantities of the Smac peptide being conjugated to the QD peptide bi-conjugate. Smac has been reported to exert its inhibitory effects on XIAP by interaction with its BIR3 domain (Arnt *et al.*, 2002 & Fandy *et al.*, 2008), therefore, with the possibility that an insufficient concentration of Smac being used, may have resulted in suboptimal inhibitory action on XIAP; subsequently, low levels of caspase 3 displacement occurred and therefore, no synergistic anti-cancer activity was observed.

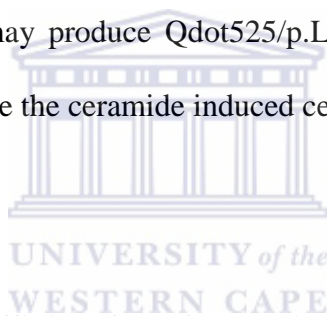
Under the same conditions, HeLa cells appear to be more susceptible to ceramide induced cell death (10 % cell viability) as compared to HT29 cells (45 % cell viability). However, again an inhibitory effect was observed when treated with the Qdot525/p.L+Smac bi-conjugates and ceramide (31 % cell viability). Therefore, suggesting that the Qdot525 targeted drug delivery system together with ceramide failed to induce a synergistic anti-cancer effect.

There were no statistically significant differences observed between the Cys-QD/p.L+Smac bi-conjugate (45 % cell viability) and the ceramide only control (36 % cell viability) for HT29 cells. Since the Cys-QDs surface chemistry is different from that of the Qdot525, in that there is no polymer coating, the potential interaction observed for the QD525/p.L+Smac bi-conjugate may be absent in Cys-QD/p.L+Smac bi-conjugate. Therefore, no cytoprotection was conferred in HT29 cells. Under the same conditions, HeLa cells showed more susceptibility to ceramide only induced cell death (12 % cell viability) as compared to HT29 cells (36 % cell viability). There were no statistically significant differences in the response of HeLa cells to the treatment with ceramide and the Qdot525/p.L+Smac bi-conjugate (31 % cell viability) as well as the Cys-QD/p.L+Smac bi-conjugate (45 % cell viability). The general observations for the HeLa cell line were greater susceptibility to cell death induced by the Qdot525/p.L+Smac and Cys-QD/p.L+Smac in the presence and absence of ceramide. This may be explained by the fact that a dose response trial was not carried out for HeLa cells and thus, the LD₅₀ for this cell line may have been lower.



In a study carried out by Fandy *et al.*, it was demonstrated that the level of IAP expression in various tumour types determines how the cancer cells will respond to the Smac peptide. The N-terminal Smac peptide was only able to sensitise low expressing IAP cancer cells; whereas it was able to induce apoptosis in high expressing IAP cancer cells (Fandy *et al.*, 2008). Furthermore, Emjedi *et al.*, showed that HT29 and HeLa cells are low expressing XIAP cell lines (Emjedi *et al.*, 2013), therefore, it is possible that the expression level of IAPs in HT29 cells were insufficient to induce sensitising to apoptosis and consequently, no synergistic anti-cancer activity was observed. In this instance, the targeted drug delivery system developed in this study will prove to be ineffective.

Alternatively, it is known that the targeting function of the Smac peptide is elicited by the first four amino acids at its N-terminal (Wu *et al.*, 2000 & Gao *et al.*, 2007 & Martinez-Ruiz *et al.*, 2008) and thus, the seemingly poorly controlled bi-conjugation setup in this study may have resulted in the bi-conjugation of the Smac peptide (N-terminal) to the p.L peptide (C-terminal), produced by EDC chemistry. The aim of using EDC chemistry was to exclude potential cross-reactivity by producing directly complexed QD peptide bi-conjugates (Herman, 2008); however, since EDC serves to complex any available carboxylic group to any available amine group, the possible peptide-peptide (p.L-Smac) product may have instigated an obstruction at the binding site of the Smac peptide, rendering Smac inactive. Therefore, the use of an alternative bi-conjugation scheme or the incorporation of a linker sequence (Fandy *et al.*, 2008) may produce Qdot525/p.L+Smac or Cys-QD/p.L+Smac bi-conjugates that are able to enhance the ceramide induced cell death.



3.11.5. Evaluating the binding affinity of the QD peptide bi-conjugates

The objective of this section was to assess and compare the binding affinity of (1) the Qdot525 peptide bi-conjugates and (2) Cys-QD peptide bi-conjugates to HT29 and HeLa cells. To undertake this, HT29 and HeLa cells were cultured and seeded as described in **Section 3.5.1 and 3.5.3**. Since the QDs offer good fluorescent properties, the QDs were used to quantify the fluorescence intensity, indicative of the QD peptide bi-conjugate binding to the cells.

Figure 3.5 and 3.6 shows the binding of the Qdot525 peptide bi-conjugates and the Cys-QD peptide conjugates to HT29 and HeLa cells, respectively. There were no significant differences between the manner in which the unconjugated QDs and the respective QD

peptide bi-conjugates stained the cells. Firstly, this data suggests that the untargeted QDs are able to penetrate the cellular membrane, which is in agreement with Cho *et al.*, who reports that the cellular uptake of free nanoparticles are attributed to their small size range and therefore permits internalisation of nanoparticles with great ease (Cho *et al.*, 2008). Secondly, this data suggests that selective targeting was not achieved. EDC served to directly complex the QD peptide bi-conjugates (Herman, 2008); however, the results suggest that this may not have been an appropriate method of bi-conjugation.

The targeting function of the p.L peptide may have been elicited by its C-terminal and thus, the close proximity of the QDs to the p.L peptide, produced by EDC, may have resulted in the loss of the p.L peptide's ability to target the erbB-2 receptor. Therefore, the use of an alternative bi-conjugation scheme or the incorporation of a linker sequence may produce a bi-conjugate that is able to target efficiently. From the literature, very efficient targeting using the p.L peptide has been demonstrated; an example of this was reported by Jie *et al.*, (2012) who used EDC bi-conjugation chemistry. However, to ensure more efficient targeting devoid of interference with the binding affinity and specificity, the p.L peptide was PEGylated (Jie *et al.*, 2012).

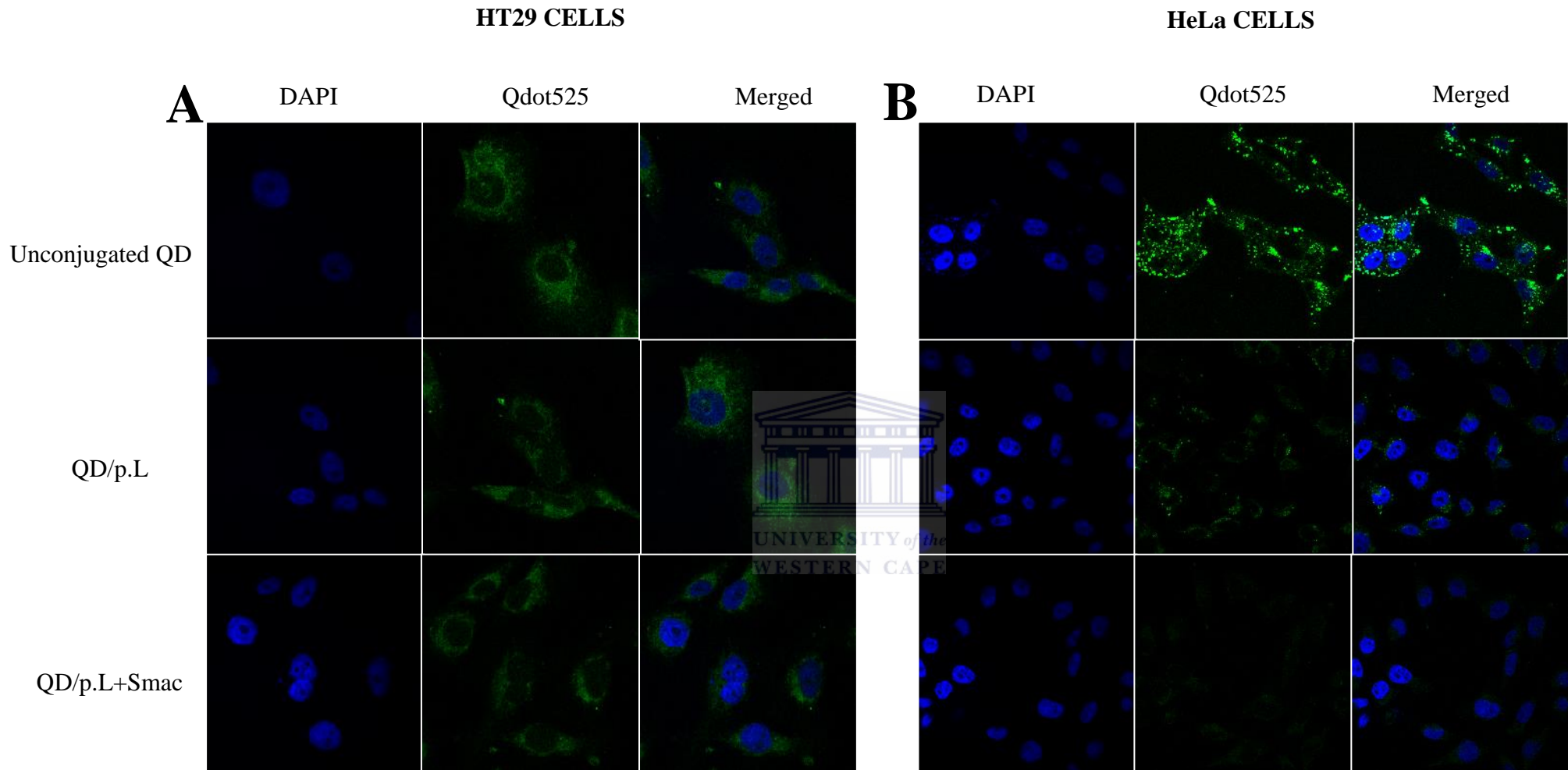


Figure 3.5. Binding of the Qdot525 peptide bi-conjugates. (A) HT29 and (B) HeLa cells were incubated with the respective Qdot525 peptide bi-conjugates for 1 hr and then counterstained with DAPI. Subsequently, the cells were examined under a confocal laser scanning microscope. Representative micrographs illustrate binding of the Qdot525 peptide bi-conjugates (green) and nuclei localisation (blue) in both cell lines. Images were captured at 100X magnification.

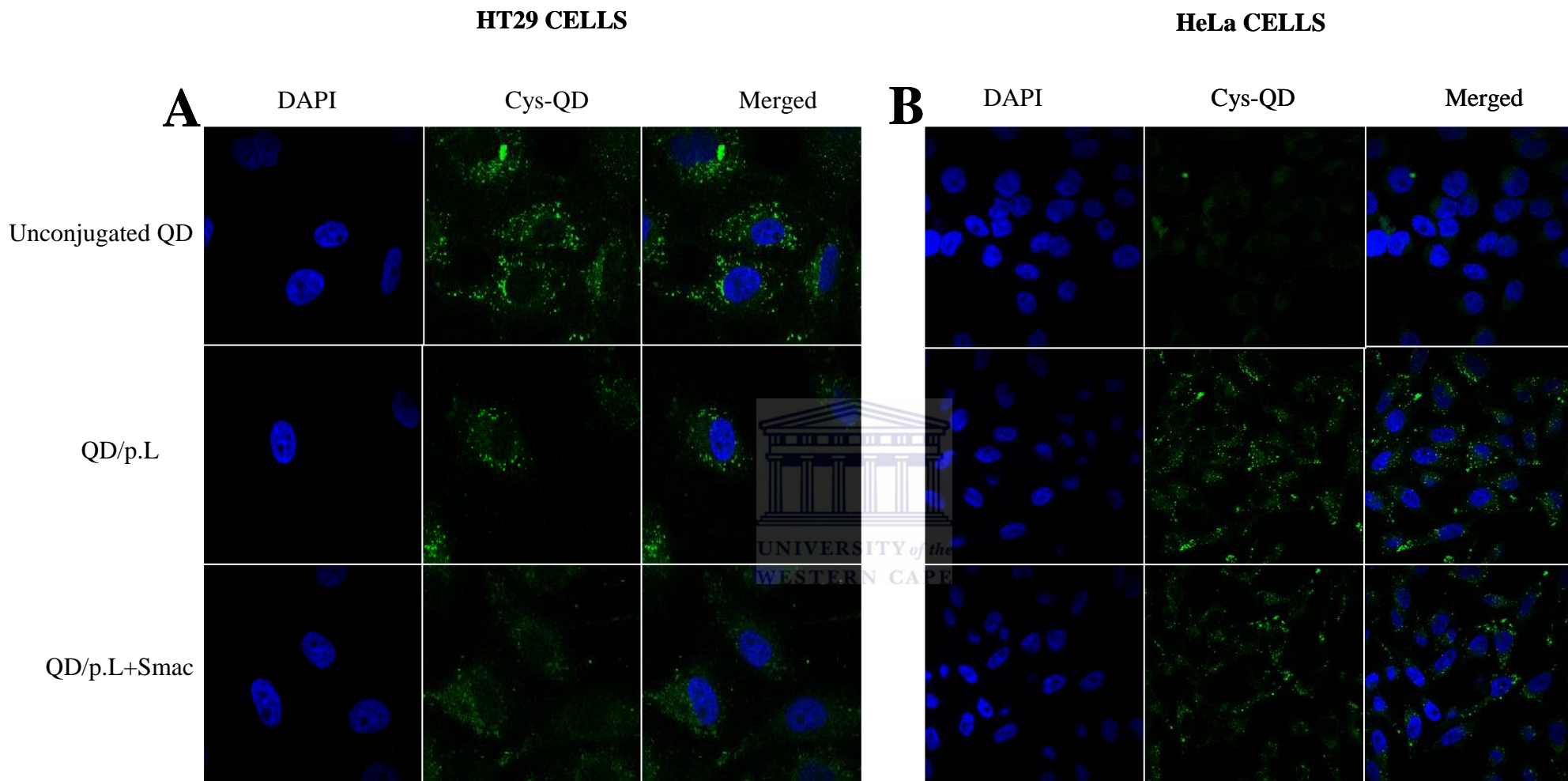
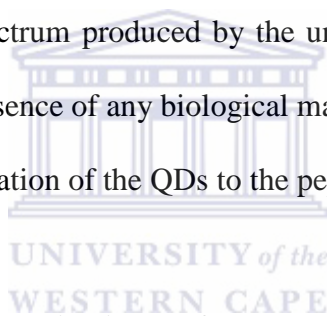


Figure 3.6. Binding of Cys-QD peptide bi-conjugates. (A) HT29 and (B) HeLa cells were incubated with the respective Cys-QD peptide bi-conjugates for 1 hr and then counterstained with DAPI. Subsequently, the cells were examined under a confocal laser scanning microscope. Representative micrographs illustrate binding of the Cys-QD peptide bi-conjugates (green) and nuclei localisation (blue) in both cell lines. Images were captured at 100X magnification.

Alternatively, the poor selectivity presented by the p.L peptide in this study may be explained by the possibility that the bi-conjugation may have been unsuccessful. This would explain why there were no significant differences observed by the manner in which the unconjugated QDs and the QD peptide bi-conjugates stained the cells. Using tools such as PL spectroscopy and EDS, it may be possible to show that a successful bi-conjugation occurred. PL uses the principle of exposing the sample to light and the PL (emitted light) gets stimulated by a higher energy, producing an emission spectrum that may be analysed computationally (Seyhan, 2003). Any red shifted emissions from that of the unconjugated QDs would communicate an increase in the QD diameter and therefore, suggest the presence of the peptide on the QD surface and in turn, a successful bi-conjugation. EDS relies on the generation of a unique x-ray spectrum produced by the unique atomic structure ascribed to every element. Therefore, the presence of any biological materials in an elemental analysis by EDS would suggest the bi-conjugation of the QDs to the peptides.



3.11.6. Evaluating the internalisation of the bi-conjugates using live cell immunocytochemistry

The literature reports the p.L peptide being able to internalise erbB-2 positive breast cancer cells (Sioud and Mobergslien, 2012). Since HT29 cells have high expression levels of the erBb-2 receptor, the objective of this section is to determine whether the p.L peptide also internalises HT29 cells.

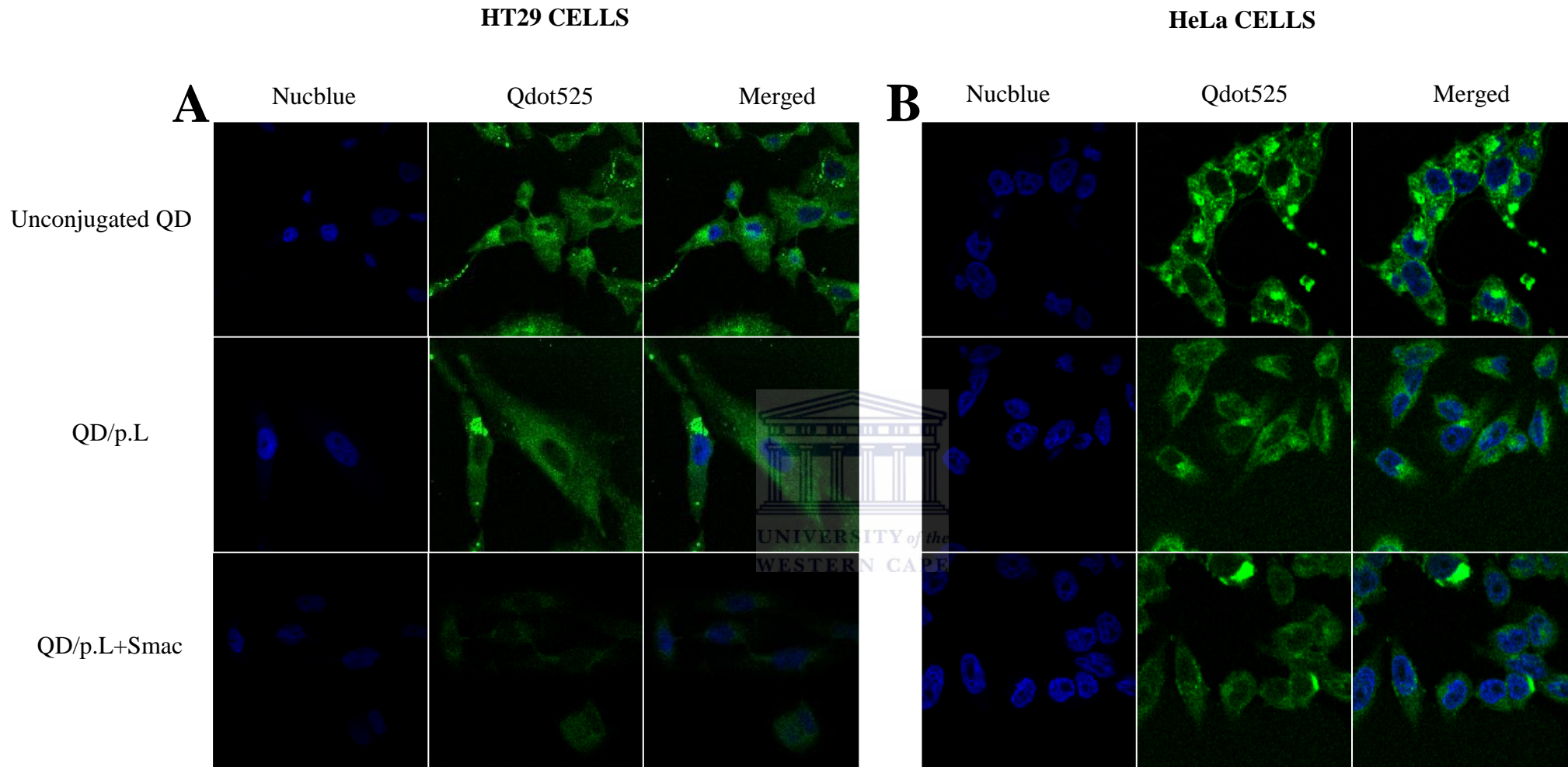


Figure 3.7. Internalisation of the Qdot525 peptide conjugates. (A) HT29 and (B) HeLa cells were incubated with the respective Qdot525 peptide bi-conjugates for 24 hrs and then counterstained with Nucblue. Subsequently, the cells were examined under a confocal laser scanning microscope. Representative micrographs illustrate efficient cellular uptake of the Qdot525 peptide bi-conjugates (green) and nuclei localisation (blue) in both cell lines. Images were captured at 100X magnification.

HT29 CELLS

HeLa CELLS

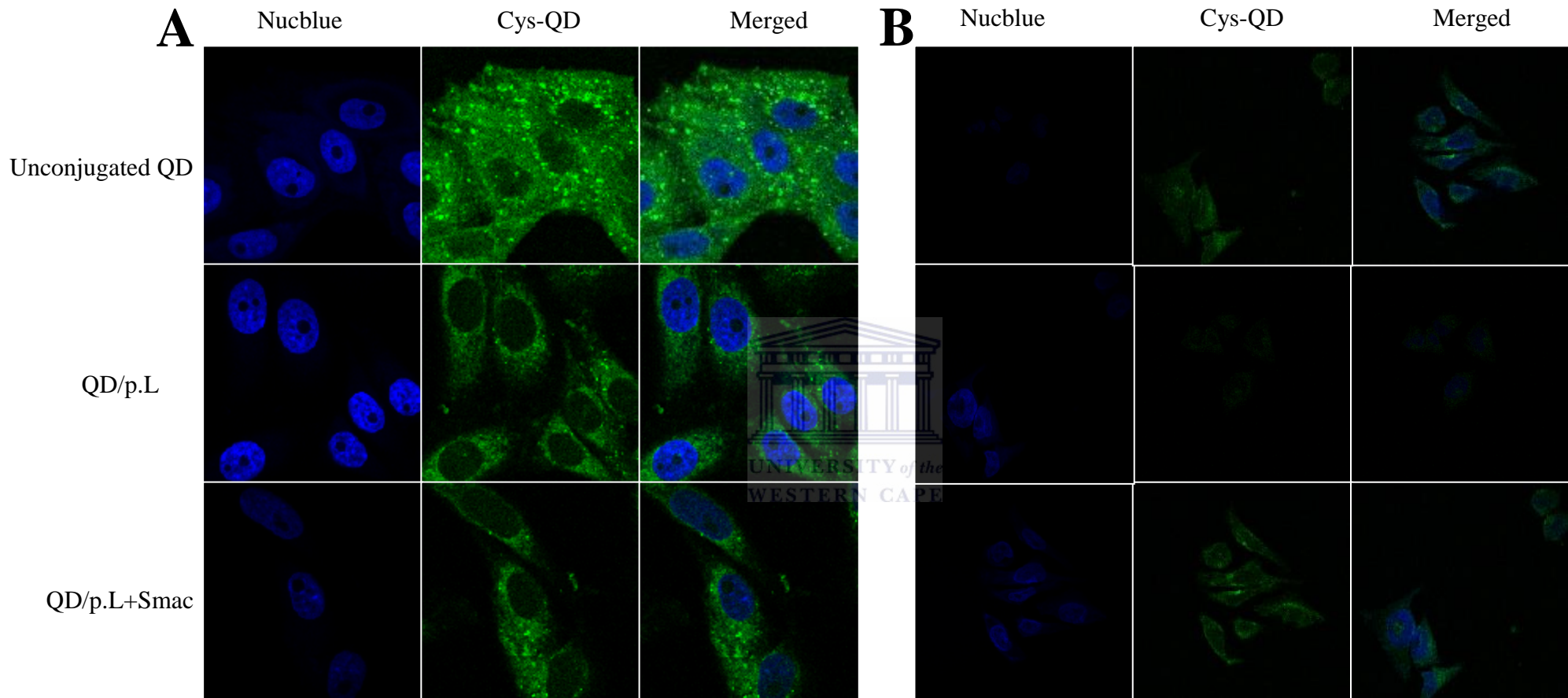
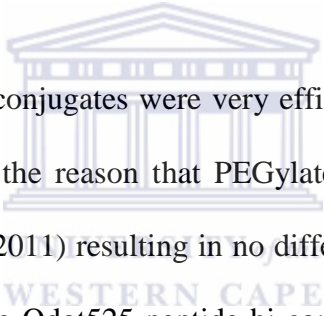


Figure 3.8. Internalisation of the Cys-QD peptide conjugates. (A) HT29 and (B) HeLa cells were incubated with the respective Cys-QD peptide bi-conjugates for 24 hrs and then counterstained with Nucblue. Subsequently, the cells were examined under a confocal laser scanning microscope. Representative micrographs illustrate efficient cellular uptake of the Cys-QD peptide bi-conjugates (green) and nuclei localisation (blue) in both cell lines. Images were captured at 100X magnification.

Figures 3.7 and 3.8 show the internalisation of the QD peptide bi-conjugates in HT29 and HeLa cells. There were no significant differences observed between the manner in which the unconjugated Qdot525 and the Qdot525 peptide bi-conjugates as well as the Cys-QD and Cys-QD peptide bi-conjugates stained the HT29 cells. This correlates with the fixed cell immunocytochemistry data (**Figure 3.5 and 3.6**) suggesting that selective targeting was not achieved. This may be due to an unsuccessful bi-conjugation, suggesting that what essentially is being observed is the staining of unconjugated QDs in all three instances (unconjugated QD or QD/p.L or QD/p.L-Smac) instead of the expected QD peptide bi-conjugates. Therefore, it would be advisable to establish whether the bi-conjugation in this study has been successful using the techniques previously discussed.



Of note, the Qdot525 peptide bi-conjugates were very efficiently taken up by HeLa cells as well. This may be explained by the reason that PEGylated QDs assists with escape from endosomal trapping (Choi *et al.*, 2011) resulting in no difference in the manner in which the different cell lines internalised the Qdot525 peptide bi-conjugates due to PEGylation of the Qdot525. This in turn explains why the Cys-QD peptide bi-conjugates showed much higher fluorescence intensity in HT29 cells as compared to that of HeLa cells, indicative of very efficient internalisation to HT29 cells since the Cys-QDs were not synthesised with any polymer coating. To fairly evaluate the uptake of the QD peptide bi-conjugates developed in this study, QDs with the exact chemistry should be used.

The data from this section demonstrated efficient uptake of the QD peptide bi-conjugates, however, no selective targeting to HT29 cells were observed; this may be attributed to the previously discussed factors explained in **Section 3.11.5**. This data also corroborates results obtained for the cytotoxicity assay, in that the QD peptide bi-conjugates were not

successfully conjugated and therefore, no enhanced ceramide induced cell death was observed in the presence of the Qdot525/p.L+Smac or Cys-QD/p.L+Smac bi-conjugates and in fact, what was observed as no enhanced anti-cancer activity in **Figure 3.4** is representative of unconjugated QDs in each instance where the Qdot525/p.L+Smac or Cys-QD/p.L+Smac bi-conjugates were expected to be internalised.



Summary of this study

4.1. General Discussion

Cancer is a leading cause of death, worldwide. It is a progressive disease, in that accumulative changes occur at the genetic level. Subsequently, presenting a disease that is complex and life-threatening (Pal and Nayak, 2010). Annual projections are expected to reach approximately 16 million new mortality cases by 2020 (Thundimadathil, 2012). These statistics suggest that current therapeutic strategies appear to be less effective and therefore presenting a need for alternative therapeutic approaches (Sumer and Gao, 2008).

The non-specific distribution of conventional chemotherapeutic drugs, imposes severe toxicities, thereby restricting the drug dosages that may be administered (Wang *et al.*, 2009). Overall, the objective is to produce an effective treatment, which directly targets and kills the cancerous cells, with little to no damage inflicted on healthy cells (Brannon-Peppas and Blanchette, 2004 & Byrne *et al.*, 2008). In view of this, the therapeutic goal of chemotherapy has shifted towards targeted drug delivery systems; which have successfully been demonstrated using cancer specific peptides (Byrne *et al.*, 2008 & Haglund *et al.*, 2009 & Sioud and Mobergslien, 2012 & Thundimadathil, 2012). In particular, the p.L peptide that has been shown to successfully target several erbB-2 positive cancer cells (Shadidi and Sioud, 2002 & Shadidi and Sioud, 2003 & Wang *et al.*, 2007 & Haglund *et al.*, 2009 & Jie *et al.*, 2012).

Additionally, the application of apoptosis inhibitory peptides as potential therapeutic modalities in targeted drug delivery systems have been reported (Shadidi and Sioud, 2003). Smac/DIABLO is a pro-apoptotic peptide that is able to interact with IAPs, thereby inducing pro-apoptotic signalling (Wu *et al.*, 2000). It has been demonstrated in literature that

Smac/DIABLO and N-terminal Smac-derived short peptides enhance the anti-cancer activity of several drugs that induce apoptosis in cancer cells (Chai *et al.*, 2000 & Arnt and Kaufmann, 2003 & Martinez-Ruiz *et al.*, 2008 & Lu *et al.*, 2011).

Nanotechnology has emerged as a promising avenue to formulate appropriate and efficient drug carriers for targeted drug delivery systems (Cao and Wang, 2011). Several nanoparticles have successfully been used in cancer treatment, of which QDs served as a delivery vehicle and imaging agent (Drbohlavova *et al.*, 2009).

QDs are fluorescent semiconductor colloidal crystalline nanoparticles with diameters, generally, ranging between 2-10 nm in size (Chan *et al.*, 1998 & Mattheakis *et al.*, 2004) and are widely being applied as imaging agents (Resch-Genger *et al.*, 2008). The unique properties exhibited by QDs are attributed to their physicochemical characteristics and therefore in the advent of synthesising these nanoparticles, determining what these characteristics are and how it plays a vital role in understanding its behaviour and subsequent application in biological systems (Zhang and Clapp, 2011).

The objective of this study was to develop a multimodal nanoparticle-based targeted drug system using peptide directed QDs as an imaging agent and delivery vehicle to selectively kill cancer cells using the pro-apoptotic peptide, Smac in combinatorial treatment with ceramide. To achieve this, highly monodispersed and green emitting fluorescent CdSe/ZnS core-shell QDs were synthesised using an organometallic approach. PL spectroscopy illustrated that the as prepared CdSe/ZnS core-shell QDs had a narrow and sharp PL spectrum, indicative of a narrow size distribution. Additionally, wavelength emissions at 525 nm were observed and therefore, suggesting green fluorescent QDs were obtained. High resolution TEM micrographs confirmed that monodispersed and spherical shaped QDs were synthesised, however, poor lattice fringes were observed, indicative of poor structural quality

QDs. The EDS analysis revealed that all four elements, Cd, Se, Zn and S were present in the as prepared QDs. The abovementioned data proved satisfactory to proceed with ligand exchange to solubilise the QDs for biological application. Water-soluble L-cysteine capped CdSe/ZnS core-shell QDs (Cys-QDs) were obtained using the method described by Carillo-Carrion *et al.*, 2009. This was established by observing the well-dispersed QDs in the aqueous solution, indicative of a successful ligand exchange.

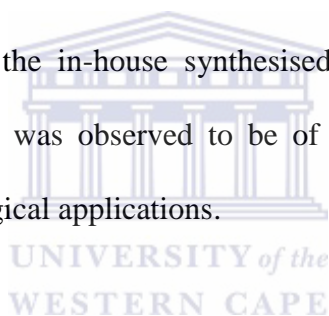
The in-house synthesised Cys-QDs and commercially available Qdot525, with similar chemistry, were used comparatively in the development of p.L peptide directed QDs functionalised with Smac. A non-hazardous dosage of the respective QDs was obtained using a dose response curve. Based on the response of HT29 cells to treatment with the QDs, it was decided to use a concentration below the LD₅₀, that is, 0.25 μ M and 350 μ g/ml for the Qdot525 and Cys-QDs, respectively. Using the aforementioned concentrations, the QDs were bi-conjugated to the p.L peptide and Smac peptide using EDC chemistry. This was followed by desalting the QD peptide bi-conjugates (Qdot525-p.L-Smac *or* Cys-QD-p.L-Smac) using PD10 gel filtration columns and the fractions with the highest fluorescence intensities were used for subsequent experiments. The potential cytotoxicity of the targeted drug delivery system developed in this study was then evaluated using the WST-1 Cell Proliferation assay. It was found that the combinatorial treatment of the Qdot525/p.L+Smac and the Cys-QD/p.L+Smac bi-conjugates did not enhance nor sensitise HT29 and HeLa cells to ceramide induced cell death. This may be explained by several factors, such as (1) insufficient concentration of Smac being used, resulting in suboptimal inhibitory action on XIAP or (2) a potential obstruction at the binding site of the Smac peptide possibly caused by bi-conjugating the peptides to each other or (3) the low expression levels of XIAP in these particular cell lines failed to sensitise the cells to apoptosis. This was confirmed when the binding affinity and internalisation of the QD peptide bi-conjugates were evaluated using

immunocytochemistry. No selective targeting to HT29 cells was observed, however, a degree of internalisation was achieved. Despite internalisation, there were no significant differences between the manner in which the respective QD peptide bi-conjugates were taken up by HT29 and HeLa cells. This was not anticipated since the literature reports that HT29 and HeLa cells retain high and low expression levels of the erbB-2 receptor, respectively (Kavanagh *et al.*, 2009). It is possible that the p.L peptide lost functionality due to the method of bi-conjugation. Additionally, the bi-conjugation may have been unsuccessful and therefore, no targeting was observed due to the absence of the targeting moiety.



4.2. Conclusion

The objective of this study was to develop a multimodal nanoparticle-based targeted drug system using peptide directed QDs as an imaging agent and delivery vehicle to selectively kill cancer cells using the pro-apoptotic peptide, Smac in combinatorial treatment with ceramide. Green fluorescent CdSe/ZnS core-shell QDs were successfully synthesised and solubilised for its application in a biological environment. This study suggests that the bi-conjugation strategy may have been unsuccessful as demonstrated by no selective targeting to HT29 cells. Additionally, the possibility of an inappropriate bi-conjugation strategy resulted in the ineffective combinatorial treatment of the QD peptide bi-conjugate and consequently, HT29 cells were not sensitised to ceramide induced cell death. Although the overall objective was not met, the efficiency of the in-house synthesised Cys-QDs in comparison to the commercially available Qdot525 was observed to be of good quality and therefore, may potentially be used in other biological applications.



4.3. Future work

Future directions would aim to address limitations identified in this study. Over time, L-cysteine forms dimers and renders the QDs insoluble in aqueous medium, thus alternative water soluble capping ligands may be investigated to produce water-soluble QDs that are stable for longer. The literature clearly demonstrates the targeting ability and apoptotic sensitising of the p.L peptide and Smac peptide, respectively. Therefore, the ineffective target drug delivery system developed in this study suggests that an unsuccessful bi-conjugation occurred, therefore, exploring alternative bi-conjugation strategies, such as the incorporation of a linker sequence to avoid the potential loss of the peptide function may be investigated. Finally, the current targeted drug delivery system should be tested on cell lines with different

levels of XIAP expression to evaluate if the conditions under which this system was developed may prove to be effective.



4.4. References

1. Allen, T.M and Cullis, P.R. (2004) 'Drug delivery systems: entering the mainstream'. *Drug Discovery*, 303, 1818 – 1822.
2. Angell, J.J. (2011) 'Synthesis and characterisation of CdSe/ZnS core-shell quantum dots for increased quantum yield'. Masters' Thesis, California Polytechnic State University, San Luis Obispo.
3. Arnt, C.R., Chiorean, M.V., Heldebrandt, M.P., Gores, G.J and Kaufmann, S.H. (2002) 'Synthetic Smac/Diablo peptides enhance the effects of chemotherapeutic agents by binding XIAP and cIAP1 in situ'. *The Journal of Biological Chemistry*, 277 (46), 44236 – 44243.
4. Arnt, C.R and Kaufmann, S.H. (2003) 'The saintly side of Smac/Diablo: giving anticancer drug-induced apoptosis a boost'. *Cell Death and Differentiation*, 10, 1118 – 1120.
5. Boatman, E.M and Lisensky, G.C. (2005) 'A safer, easier, faster synthesis for CdSe quantum dots nanocrystals'. *Journal of Chemical Education*, 82 (11), 1697 – 1699.
6. Brannon-Peppas, L and Blanchette, J.O. (2004) 'Nanoparticle and targeted systems for cancer therapy.' *Advanced Drug Delivery Reviews*, 56, 1649 – 1659.
7. Byrne, J.D., Betancourt, T and Brannon-Peppas, L. (2008) 'Active targeting schemes for nanoparticles systems in cancer therapeutics.' *Advanced Drug Delivery Reviews*, 60, 1615 – 1626.
8. Chai, J., Du, C., Wu, J.W., Kyin, S., Wang, X and Shi, Y. (2000) 'Structural and biochemical basis of apoptotic activation by Smac/diablo'. *Nature*, 406, 855 – 862.
9. Chen, N., He, Y., Su, Y., Li, X., Huang, Q., Wang, H., Zhang, X., Tai, R and Fan, C. (2011) 'The cytotoxicity of cadmium-based quantum dots'. *Biomaterials*, 33(2012), 1238 – 1244.

10. Cho, K., Wang, K and Nie, S. (2008) 'Therapeutic nanoparticles for drug delivery in cancer.' *Clinical Cancer Research*, 14, 1310 – 1316.
11. Choi, Y., Kim, K., Hong, S., Kim, H., Kwon, Y.J and Song, R. (2011) 'Intracellular protein target detection by quantum dots optimized for live cell imaging'. *Bioconjugate Chemistry*, 22, 1576 – 1586.
12. Dabbousi, B.O., Rodriguez-Viejo, J., Mikulec, F.V., Heine, J.R., Mattoussi, H., Ober, R., Jensen, K.F and Bawendi, M.G. (1997) '(CdSe)ZnS core – shell quantum dots: synthesis and characterisation of a size series of highly luminescent nanocrystallites'. *The Journal of Physical Chemistry B*, 101, 9463 – 9475.
13. Danhier, F., Feron, O and Preat, V. (2010) 'To exploit the tumor microenvironment: Passive and active tumor targeting of nanocarriers for anti-cancer drug delivery.' *Journal of Controlled Release*, 148, 135 – 146.
14. De Barros, A.L.B., Tsourkas, A., Saboury, B., Cardoso, V.N and Alavi, A. (2012) 'Emerging role of radiolabeled nanoparticles as an effective diagnostic technique.' *EJNMMI Research*, 2(39), 1 – 5.
15. Deveraux, Q.L and Reed, J.C. (1999) 'IAP family proteins - suppressors of apoptosis'. *Genes and Development*, 13, 239 – 252.
16. Duckett, C.S. (2005) 'IAP proteins: sticking it to Smac'. *Biochemical Journal*, 385, e1 – e2.
17. Emjedi, Z., Meyer, M and Madiehe, A. (2013) 'Targeted delivery of embelin to cancer cells'. Masters' Thesis, University of the Western Cape, South Africa.
18. Fandy, T.E., Shankar, S and Srivastava, R.K. (2008) 'Smac/DIABLO enhances therapeutic potential of chemotherapeutic drugs and irradiation, and sensitises TRAIL-resistant breast cancer cells'. *Molecular Cancer*, 4(60), 1 – 10.

19. Felding-Habermann, B., O'Toole, T.E., Smith, J.W., Fransvea, E., Ruggeri, Z.M., Ginsberg, M.H., Hughes, P.E., Pampori, N., Shattil, S.J., Saven, A and Mueller, B.M. (2001) 'Integrin activation controls metastasis in human breast cancer'. *PNAS*, 98(4), 1853 – 1858.
20. Ferrari, M. (2005) 'Cancer Nanotechnology: Opportunities and Challenges'. *Nature Reviews*, 5, 161 – 171.
21. Fischer, U and Schulze-Osthoff, K. (2005) 'New approaches and therapeutics targeting apoptosis in disease'. *Pharmacological Reviews*, 57, 187 – 215.
22. Fulda, S and Debatin, K.M. (2006) 'Extrinsic versus intrinsic apoptosis pathways in anticancer chemotherapy'. *Oncogene*, 25, 4798.
23. Fulda, S. (2009) 'Inhibitors of apoptosis (IAP) proteins: Novel insights into the cancer-relevant targets for cell death induction'. *ACS Chemical Biology*, 4(7), 499 – 501.
24. Gao, Z., Tian, Y., Wang, J., Yin, Q., Wu, H., Li, Y and Jiang, X. (2007) 'A dimeric Smac/Diablo directly relieves caspase-3 inhibition by XIAP'. *The Journal of Biological Chemistry*, 282 (42), 30718 - 30727.
25. Gomes, A.S.O., Vieira, C.S., Almeida, D.B., Santos-Mallet, J.R., Menna-Barreto, R.F.S., Cesar, C.L and Feder, D. (2011) 'CdTe and CdSe quantum dots cytotoxicity: A comparative study on microorganisms'. *Sensors*, 11, 11664 – 11678.
26. Grabolle, M., Ziegler, J., Merkulov, A., Nann, T and Resch-Genger, U. (2008) 'Stability and fluorescence quantum yield of CdSe-ZnS quantum dots – influence of the thickness of ZnS shell'. *Annals of the New York Academy of Sciences*, 1130, 235 – 241.
27. Guo, F., Nimmanapalli, R., Paranawithana, S., Wittman, S., Griffin, D., Bali, P., O'Bryan, E., Fumero, C., Wang, H.G and Bhalla, K. (2002) 'Ectopic overexpression

- of second mitochondria-derived activator of caspases (Smac/DIABLO) or cotreatment with N-terminus of Smac/DIABLO peptide potentiates epothilone B derivative-(BMS 247550) and APO-2L/TRAIL-induced apoptosis'. *Blood*, 99, 3419 – 3426.
28. Haglund, E., Seale-Goldsmith, M.M and Leary, J.F. (2009) 'Design of multifunctional nanomedical systems'. *Annals of Biomedical Engineering*, 1 – 16.
29. Hardman, R. (2006) 'A toxicological review of quantum dots: toxicity depends on physicochemical and environmental factors'. *Environmental Health Perspectives*, 114(2), 165 – 172.
30. Hermanson, G.T. (2008) *Bioconjugate Chemistry*. 2nd ed. London: Academic Press.
31. Hermanson, G.T. (2013) *Bioconjugate Chemistry*. 3rd ed. London: Academic Press.
32. Hines, M.A and Guyot-Sionnest, P. (1996) 'Synthesis and characterisation of strongly luminescing ZnS-capped CdSe nanocrystals'. *Journal of Physical Chemistry*, 100, 468 – 471.
33. Ho, Y.P and Leong, K.W. (2010) 'Quantum dots-based theranostics'. *Nanoscale*, 2(1), 60-68.
34. Huy, B.T., Seo, M.H., Lim, J.M., Shin, D.S and Lee, Y.I. (2011) 'A systematic study on preparing CdS quantum dots'. *Journal of the Korean Physical Society*, 59(5), 3293 – 3299.
35. Jamieson, T., Bahkshi, R., Petrova, D., Pocock, R., Imani, M and Seifalian, A.M. (2007) 'Biological applications of quantum dots'. *Biomaterials*, 28, 4717 – 4732.
36. Jaracz, S., Chen, J., Kuznetsova, L.V and Ojima, I. (2005) 'Recent advances in tumor –targeting anticancer drug conjugates'. *Bioorganic and Medicinal Chemistry*, 13(2005), 5043 – 5054.

37. Jones, M., Nedeljkovic, J., Ellingson, R.J., Nozik, A.J and Rumbles, G. (2003) 'Photoenhancement of luminescence in colloidal CdSe quantum dot solution'. *Journal of Physical Chemistry*, 107, 11346 – 11352.
38. Jie, L.Y., Cai, L.L., Wang, L.J., Ying, X.Y., Yu, R.S and Du, Y.Z. (2012) 'Actively targeted LTVSPWY peptide modified magnetic nanoparticles for tumor imaging'. *International Journal of Nanomedicine*, 7, 3981 – 3989.
39. Jin, S., Hu, Y., Gu, Z., Liu, L and Wu, H.C. (2011) 'Application of quantum dots in biological imaging'. *Journal of Nanomaterials*, 2011, 1 – 13.
40. Li, Z.L and Cho, C.H. (2012) 'Peptides as targeting probes against tumor vasculature for diagnosis and drug delivery'. *Journal of Translational Medicine*, 10, 1 – 9.
41. Li, J., Wu, D., Miao, Z and Zhang, Y. (2010) 'Preparation of quantum dots bioconjugates and their applications in bio-imaging'. *Current Pharmaceutical Biotechnology*, 11, 662 – 671.
42. Liu, W., Choi, H.S., Zimmer, J.P., Tanaka, E., Frangioni, J.V and Bawendi, M. (2007) 'Compact cysteine-coated CdSe(ZnCdS) quantum dots for in vivo applications'. *Journal of American Chemical Society*, 129, 14530 – 14531.
43. Lu, J., McEachern, D and Sun, H. (2011) 'Therapeutic potential and molecular mechanism of a novel, potent, nonpeptide, Smac mimetic SM-164 in combination with TRAIL for cancer treatment'. *Molecular Cancer Therapeutics*, 10, 902 – 914.
44. Lu, R.M., Chen, M.S., Chang, D.K., Chiu, C.Y., Lin, W.C., Yan, S.L., Wang, Y.P., Kuo, Y.S., Yeh, Y.S., Yeh, C.Y., Lo, A and Wu, H.C. (2013) 'Targeted drug delivery systems mediated by a novel peptide in breast cancer therapy and imaging'. *PLOS one*, 8(6), 1 – 3.

45. Martinez-Ruiz, G., Maldonado, V., Ceballos-Cancino, G., Grajeda, J.P.R and Melendez-Zajgla, J. (2008) 'Role of Smac/Diablo in cancer progression'. *Journal of Experimental and Clinical Cancer Research*, 27(48), 1 – 7.
46. Medintz, I.L., Uyeda, H.T., Goldman, E.R and Mattoussi, H. (2005) 'Quantum dot bioconjugates for imaging, labelling and sensing'. *Nature Materials*, 4, 435 – 446.
47. Nichols, J.W and Bae, Y.H. (2012) 'Odyssey of a cancer nanoparticle: From injection site to site of action'. *Nano Today*, 7, 606 – 618.
48. Normanno, N., De Luca, A., Bianco, C., Strizzi, L., Mancino, M., Maiello, M.R., Carotenuto, A., De Feo, G., Caponigro, F and Salomon, D, S. (2005) 'Epidermal growth factor receptor (EGFR) signalling in cancer'. *Gene*, 366(2006), 2 – 16.
49. Nguyen, K.T. (2011) 'Targeted nanoparticles for cancer therapy: promises and challenges.' *Journal of Nanomedicine and Nanotechnology*, 2(5), 1 – 2.
50. Oudhia, A. (2012) 'UV-Vis spectroscopy as a non-destructive and effective characterisation tool for II-VI compounds'. *Recent Research in Science and Technology*, 4(8), 109 – 111.
51. Pal, D and Nayak, A.M. (2010) 'Nanotechnology for targeted delivery in cancer therapeutics.' *International Journal of Pharmaceutical Sciences Review and Research*, 1(1), 1 – 7.
52. Pechstedt, K., Whittle, T., Baumberg, J and Melvin, T. (2010) 'Photoluminescence of colloidal CdSe/ZnS quantum dots: The critical effect of water molecules.' *Journal of Physical Chemistry*, 114, 12069 – 12077.
53. Pong, B.K., Trout, B.L and Lee, J.M. (2008) 'Modified ligand exchange for efficient solubilisation of CdSe/ZnS quantum dots in water: A procedure guided by computational studies'. *American Chemical Society*, 24, 5270 – 5276.

54. Qi, L., Colfen, H and Antonietti, M. (2000) 'Synthesis and characterisation of CdS nanoparticles stabilised by double-hydrophilic block copolymers'. *Nanoletters*, 1(2), 61 – 65.
55. Rajalingam, K., Oswald, M., Gottschalk, K and Rudel, T. (2007) 'Smac/Diablo is required for effector caspase activation during apoptosis in human cells'. *Apoptosis*, 12, 1503 – 1510.
56. Rao, C.N.R and Biswas, K. (2009) 'Characterisation of nanomaterials by physical methods'. *Annual Review of Analytical Chemistry*, 2, 435 – 462.
57. Reiss, P., Protiere, M and Li, L. (2009) 'Core/shell semiconductor nanocrystals'. *Small*, 5(2), 154 – 168.
58. Resch-Genger, U., Grabolle, M., Calaviere-Jaricot, S., Nitschke, R and Nann, T. (2008) 'Quantum dots versus organic dyes as fluorescent labels'. *Nature Methods*, 5 (9), 763 – 775.
59. Seyhan, A. (2003) 'Photoluminescence Spectroscopy of CdS and GaSe'. Masters' Thesis, The Graduate School of Natural and Applied Science of The Middle East Technical University, The Middle East.
60. Shadidi, M and Sioud, M. (2002) 'Identification of novel carrier peptides for the specific delivery of therapeutics into cancer cells'. *The FASEB Journal*, 1, 1 – 17.
61. Shadidi, M and Sioud, M. (2003) 'Selective targeting of cancer cells using synthetic peptides'. *Drug Resistance Updates*, 6(2003), 363 – 371.
62. Shiozaki, E.N and Shi, Y. (2004) Caspases, IAPs and Smac/Diablo: mechanisms from structural biology. 'TRENDS in Biochemical Sciences', 39 (9), 486 – 494.
63. Singh, R and Lillard Jr, J.W. (2009) 'Nanoparticle-based targeted drug delivery'. *Experimental and Molecular Pathology*, 86(3), 215 – 223.

64. Sinha, R., Kim, G.J., Nie, S., shin, D.M. (2006) 'Nanotechnology in cancer therapeutics: bioconjugated nanoparticles for drug delivery'. *Molecular Cancer Therapeutics*, 5(8): 1909 – 1917.
65. Sioud and Mobergslie (2012) 'Selective killing of cancer cells by peptide-targeted delivery of an anti-microbial peptide'. *Biochemical Pharmacology*, 84(2012), 1123 – 1132.
66. Steichen, S.D, Caldorera-Moore, M. and Peppas, N.A. (2012) 'A review of current nanoparticle and targeting moieties for the delivery of cancer therapeutics'. *European Journal of Pharmaceutical Sciences*, 48(2013), 416 – 427.
67. Sumer, B and Gao, J. (2008) 'Theranostic medicine for cancer.' *Nanomedicine*, 3(2), 137 – 140.
68. Svensen, N., Walton, J.G.A. and Bradley, M. (2012) 'Peptides for cell-selective drug delivery'. *Trends in Pharmacological Sciences*, 33(4), 186 – 192.
69. Takeuchi, H., Kim, J and Fujimoto, A. (2005) 'X-linked inhibitor of apoptosis protein expression level in colorectal cancer is regulated by hepatocyte growth factor/c-met pathway via Akt signalling'. *Clinical Cancer Research*, 11, 7621 – 7628.
70. Tamm, I., Kornblau, S.M and Segall, H. (2000) 'Expression and prognostic significance of IAP-family genes in human cancers and myeloid leukemias'. *Clinical Cancer Research*, 6, 1796 – 1803.
71. Thundimadathil, J. (2012) 'Cancer treatment using peptides: Current therapies and future prospects'. *Journal of Amino Acids*, 2012, 1 – 13.
72. Tiwari, D.K., Tanaka, S.I., Inouye, Y., Yoshizawa, K., Watanabe, T.M and Jin, T. (2009) 'Synthesis and characterisation of anti-her2 antibody conjugated CdSe/ZnS quantum dots for fluorescence imaging of breast cancer cells.' *Sensors*, 9, 9332 – 9354.

73. Vashist, S.K. (2012) 'Comparison of 1-ethyl-3-(3dimethylaminopropyl) carbodiimide based strategies to crosslink antibodies on amine-functionalised platforms for immunodiagnostic applications'. *Diagnostics*, 2, 23 – 33.
74. Vasir, J.K., Reddy, M.K., Labhsetwar, V.D. (2005) 'Nanosystems in drug targeting: Opportunities and challenges.' *Current Nanoscience*, 1, 47 – 64.
75. Wang, X.F., Witting, P.K., Salvatore, B.A and Neuzil, J. (2005) 'Vitamin E analogs triggers apoptosis in Her2/erbB2-overexpressing breast cancer cells by signalling via the mitochondrial pathway'. *Biochemical and Biophysical Research Communications*, 326(2005), 282 – 289.
76. Wang, X.F., Birringer, M and dong, L.F. (2007) 'A peptide conjugate of vitamin e succinate targets breast cancer cells with high erbB-2 expression'. *Cancer Research*, 67, 3337 – 3344.
77. Wang, X., Yang, L., Chen, Z and Shin, D.M. (2008) 'Application of nanotechnology in cancer therapy and imaging.' *A Cancer Journal for Clinicians*, 58, 97 – 110.
78. Wang, X., Wang, Y., Chen, Z.G and Shin, D.M. (2009) 'Advances of cancer therapy by nanotechnology'. *Cancer Research Treatment*, 41(1), 1 – 11.
79. Wei, Y., Fan, T and Yu, M. (2008) 'Inhibitor of apoptosis proteins and apoptosis'. *Acta Biochimica Biophysica Sinica*, 40 (4), 278 – 288.
80. Wilkinson, J.C., Wilkinson, A.S., Scott, F.L., Csomos, R.A., Salvesen, G.S and Duckett, C.S. (2004) 'Neutralisation of Smac/Diablo by inhibitors of apoptosis (IAPs): A caspase –independent mechanism for apoptotic inhibition'. *The Journal of Biological Chemistry*, 279 (49), 51082 – 51090.
81. Winnik, F.M and Maysinger, D. (2012) 'Quantum dots cytotoxicity and ways to reduce it'. *Accounts of Chemical Research*, 46(3), 672 – 680.

82. Wu, G., Chai, J., Suber, T.L., Wu, J.W., Du, C., Wang, X and Shi, Y. (2000) 'Structural basis of IAP recognition by Smac/Diablo'. *Nature*, 408, 1008 – 1012.
83. Xing, Y and Rao, J. (2008) 'Quantum dot bioconjugates for *in vitro* diagnostics & *in vivo* imaging'. *Cancer Biomarkers*, 4, 307 – 319.
84. Xu, H., Yu, Y and Marciniak, D. (2005) 'Epidermal growth factor receptor (EGFR)-related protein inhibits multiple members of the EGFR family in colon and breast cancer cells'. *Molecular Cancer Therapeutics*, 4, 435 – 442.
85. Yong, K.T., Ding, H., Roy, I., Law, W.C., Bergey, E.J., Maitra, A and Prasad, P.N. (2009) 'Imaging pancreatic cancer using bioconjugated InP quantum dots'. *ACS Nano*, 3 (3), 502 – 510.
86. Yu, M.K., Park, J and Jon, S. (2012) 'Targeting strategies for multifunctional nanoparticles in cancer imaging and therapy.' *Theranostics*, 2(1), 3 – 44.
87. Zhang, Y and Clapp, A. (2011) 'Overview of stabilising ligands for biocompatible quantum dot nanocrystals'. *Sensors*, 11, 11036 – 11055.
88. Zeng, R., Zhang, T., Liu, J., Hu, S., Wan, Q., Liu, X., Peng, Z and Zou, B. (2009) 'Aqueous synthesis of type II CdTe/CdSe core-shell quantum dots for fluorescent probe labelling tumor cells'. *Nanotechnology*, 20, 1 – 8.
89. Zhang, L., Gu, F.X., Chan, J.M., Wang, A.Z., Langer, R.S and Farokhzad, O.C. (2008) 'Nanoparticles in medicine: Therapeutic applications and developments'. *Clinical Pharmacology and Therapeutics*, 83 (5), 761 – 769.
90. Zou, Y., Li, D and Yang, D. (2010) 'Noninjection synthesis of CdS and alloyed CdS_xSe_{1-x} nanocrystals without nucleation initiators'. *Nanoscale Res Letters*, 5, 966 – 971.